Super-MAC: Data Duplication and Combining for Reliability Enhancements in Next-Generation Networks

ABDUL MATEEN AHMED[ID], **(Graduate Student Member, IEEE), AAQIB PATEL**[ID]**, (Member, IEEE), AND MOHAMMED ZAFAR ALI KHAN**[ID]**, (Senior Member, IEEE)**
Department of Electrical Engineering, Indian Institute of Technology Hyderabad, Hyderabad 502285, India
Corresponding author: Aaqib Patel (aaqib@iith.ac.in)

ABSTRACT A piece of user equipment (UE), typically, has access to multiple radio access technologies (RATS). Moreover, apart from the standard primary cellular network, the secondary cellular networks can assist the primary network in downlink UE communications. In this way, the data can reach the UE through multiple entities. This paper exploits the multiple entities' idea by proposing a cross-layer scheme that combines data to improve the block error rate (BLER) and the throughput. For this, we define a new entity, called the super-MAC, just above the Medium Access Control (MAC) layer. More specifically, we propose data duplication (at the transmitter) and combining (at UE) at the super-MAC, where the super-MAC gets the Radio Link Layer protocol data unit (RLC-PDU) and sends multiple-copies across various interfaces to different MAC-entities. In doing so, the super-MAC attaches a unique sequence number to a group of RLC-PDUs together. At the UE, the data from different MAC entities are combined at super-MAC to clear any block error. The super-MAC operates in between the Cyclic Redundancy Check and Forward Error Correction stages of the HARQ process. The additional complexity introduced by the scheme is negligible in front of the existing operations. Moreover, the average latency improves due to the significant improvement in the Block Error rate (BLER) that the combining scheme offers over the BLER of the conventional standalone system. Also, since the errors significantly reduce, the throughput shows significant improvement. Finally, the proposed scheme is an advancement in HARQ to reduce retransmissions, and hence it is suitable for the next-generation networks like B5G or 6G to adopt the super-MAC.

INDEX TERMS Diversity, super-MAC, data duplication, data combining, BLER, throughput, 4G-LTE, WiFi, latency, 5G-NR, B5G networks.

I. INTRODUCTION

With an increase in the number of users, there has been an exponential increase in demand for data, which has caused tremendous pressure on the current cellular networks like 4G-LTE and non-standalone 5G-NR. In the future, the 5G-NR based networks will also face tremendous pressure to meet user requirements, primarily because of the scarcity of vacant sub-6 GHz bandwidth where the transceiver design is relatively more manageable than the high mmWave frequencies. The B5G networks need to enhance reliability to reduce the redundant reuse due to retransmissions.

The associate editor coordinating the review of this manuscript and approving it for publication was Matti Hämäläinen[ID].

The 3GPP has sought to utilize the unlicensed band in the sub-6 GHz range, where the widely used IEEE 802.11xx standards operate. Hence, the 3GPP has primarily shown interest in operating at these frequencies in harmony with IEEE 802.11xx or WiFi technology with three primary approaches. Firstly, the LTE-unlicensed (LTE-U) or licensed assisted access (LAA), where LTE operates in the unlicensed bands [1] either with sensing the WiFi signals before transmitting (listen-before-talk) [2]–[4], with orthogonal existence [5] or with fair existence [6]–[8]. Deep-learning based resource management for fair coexistence of LTE and WiFi [9] is proposed in [9]. However, there are many challenges which need to be addressed [10], [11] including ensuring interference management and power control.

Such approaches are also suggested for the 5G-NR (NR-U) [12]–[14]. The second approach is the LTE-WiFi Aggregation (LWA), where packet data protocol convergence (PDCP) layer splits the data at the eNodeB and sends part of the data from the eNodeB to the UE directly and offloads the other part to the WiFi-access point (AP) through the *Xw* interface and finally to the UE [4], [15]–[18]. Splitting of data can be performed [19], [20] or the data can be switched among the LTE and WiFi depending upon which path performs better [21]. Commercial deployment scenarios are also considered for LWA [22]. The Aggregation of NR with WiFi is also an active area of research [23], [24]. Finally, the third approach is the LTE-WiFi integration through secured IP tunnelling where the IP layer sends the data across either to LTE or WiFi from the IP layer [15], [25]–[27]. Note that these approaches' central idea is enhancing the achievable throughput by offloading some of the traffic to WiFi from LTE. In particular, the data sent across LTE and WiFi are distinct. LWA works because the UE can arrange the PDCP protocol data units (PDUs), that have traversed two different paths, in the correct order using the appropriate SN.

The 3GPP has also prescribed dual connectivity to provide non-standalone access for 5G-NR, where the 5G cells are connected to 4G core network [28], [29].

Only recently, in release 15 [30], has attention also been given to PDCP layer data duplication, where the same PDCP PDU is duplicated and sent through different RLC entities with the aim to achieve reliability. The different RLC PDUs can use the same MAC entity through carrier aggregation or pass through completely different MACs [31]. Using multi-RAT connectivity, the PDCP PDU can be duplicated and passed through different RATs through the *Xw* interface. The primary aim of duplication is achieving reliability [32]–[35] for URLLC applications. It is also proposed for video applications through a network coding framework at the PDCP layer [36].

The PDCP duplication has its own set of challenges [37]. So far, the works that have addressed PDCP duplication accept data only from one path and discard the other, which is feasible as long as one of the paths achieves reliable communication. However, when all the paths (two in the simplest case) fail, then compulsory retransmission of the entire block is required. Given that the round trip time is a significant number over other fixed processing delays, the latency can increase [33]. Also, since the PDCP sits at the top of the L2 layer, the cross-layer scheme has relatively more computation complexity. Hence, performing operations similar to LWA offloading, but at the RLC layer [38] are also reported.

Note that the HARQ process sits below the RLC layer. Thus any modifications to this would need to be addressed below this layer. There are two steps in HARQ first, where the physical layer performs a cyclic redundancy check to detect errors. Second, where forward error correction procedure which corrects the some fixed number of errors. It is well-known that FEC is an expensive procedure, both computationally as well as in terms of bandwidth. However, without

FEC the round trip times that result from retransmissions are quite severe and increase the latency beyond current specifications. Hence, a scheme that relies less on FEC for error correction and computationally cheaper is needed.

In this paper, we propose data duplication and combining schemes at a newly defined entity, super-MAC. The super-MAC sits between the RLC and the MAC layer of the primary network, and can hence be part of the HARQ process. The super-MAC supplies the same version of the data and the essential control information to the secondary MAC entities. At the receiver, the super-MAC receives data from all the MAC entities. If any MAC entity has reported a successful reception of data, then the super-MAC discards other users' data. However, if all the MAC entities declare a failed CRC check, the super-MAC combines the data and provides the primary MAC with the combined version of the correct data before proceeding for FEC at the primary MAC entity. This combined version is likely to be less corrupted than the original corrupted version. The redundancy used in the coding scheme to correct the combined packet can be significantly less than that in the standalone scenario. Thus the overhead associated with FEC can be significantly reduced. The usage of super-MAC is shown to improve the BLER and enhance the throughput. These schemes will offer cell edge users with better reliability and other users with power savings for a given target BLER. Also, in many practical regimes of interest, our scheme offers better latency performance.

Against this background, the following are our contributions in this paper:

- We first present the super-MAC based combining scheme and derive the optimal rule when soft-bits or log-likelihood ratios (LLRs) are combined that minimizes the bit errors.
- When soft-bits are not available, we suggest a hard-combining scheme with the same performance as the selection combining scheme. We analytically derive the block error rate and highlight the improvement achieved by combining data for hard-combining.
- We take an example of LTE assisted by WiFi. Using simulations, we demonstrate the performance gains achieved in terms of BLER and throughput for both the hard-combining and soft-combining schemes. Also, we study the impact on latency due to combining data. The average round-trip-times decrease significantly because of substantial improvement in the BLER, while the increase in fixed one-way latency due to super-MAC is negligible, resulting in improved average latency.
- We also take examples of NR-LTE, NR-WiFi and LTE-WiFi and compare our combining scheme's performance, with the PDCP based duplication scheme. We show that combining at the super-MAC is superior to PDCP based approach in terms of BLER and throughput.
- We discuss that our scheme essentially plays an important role in reducing re-transmissions and sits between

the CRC and the FEC stages of the HARQ process. Thus this new addition reduces the complexity that is associated with FEC while also ensuring good reliability performance.

The rest of the paper is as follows. We first discuss the different LTE (NR) and WiFi Coexistence mechanisms in Section II. We then introduce a generic theoretical model of the system in Section III. We follow with the description of the super-MAC combining scheme in Section IV. We derive analytical expressions for the BLER in Section V and analyse the Latency in Section VI. Next, we describe the two combining scenarios in Section VII-A. We present the simulation results and their interpretation in Section IX. Finally we conclude in Section X.

II. LTE-U, LAA, MULTEFIRE, LWA, LWIP

This section summarises the various approaches adopted to meet the exponential growth in cellular traffic in 3GPP networks. Although these approaches speak of LTE and WiFi coexistence mechanisms, they are essentially coexistence of 3GPP networks with WiFi. Hence, instead of LTE, these may very well be 5G-NR or even B5G networks.

A. LTE-U AND LAA

In LTE-U, LTE operates in the unlicensed band. Originally, Qualcomm designed LTE-U to work in regions which do not mandate the "listen before talk" (LBT) protocol. LBT [39], [40] refers to a procedure that checks for ongoing transmissions in the unlicensed band, and essentially avoids interference and improves spectral efficiency. Hence, regulations in Europe and Japan mandate the use of LBT in unlicensed bands.

To incorporate this and provide a globally deployable solution that could, the 3GPP in its release 13 [1], [41] has proposed LTE in the unlicensed band equipped with LBT and termed it as Licensed Assisted Access (LAA). The unlicensed transmission for the licensed user will be governed by the 3GPP standard [42] which is being studied and continually updated. Note that similar to LTE-U, NR-U is also under active consideration for operations of NR in unlicensed band [43].

The new standard IEEE 802.11ax allows multi-user transmission by partitioning the frequency band into a substantially large number of resource units. Thus the 3GPP networks have to perform LBT at all frequencies in the band and not merely calculate the whole band's energy. Hence, careful mechanisms that need to be adaptive [44], robust [45], and fair [6] have to be designed for LBT considering the incumbent traffic in these unlicensed band.

LAA has shown promising results in significantly improving throughput. However, when LAA employs multiple secondary base stations (LTE-eNBs) as in dense deployments, LBT tends to hinder WiFi operations and hence it is necessary to check on the density of deployment, and the LTE frame structure [39]. It has also led to suggestions of a more

dramatic approach of MulteFire that allows standalone LTE operations in the unlicensed band.

B. MulteFire

MulteFire and its enhancement, the eMTC-U, suggested by the MulteFire-forum, operates in a standalone fashion in an unlicensed or shared medium [46]. It can be useful for an easy-to-deploy scenario that uses the WiFi APs to route cellular traffic [47]. Multefire dramatically increases the throughput; however, because of the scarcity of available bandwidth, it saturates relatively fast [48]. Nevertheless, it can improve system capacity and coverage in some specific environments, and small cell deployments [49]. Moreover, it is a possible candidate for deploying the massively connected Narrow-Band IoT [50] as well as more massive-Machine Type communications (mMTC) [51].

Also, in the newer releases that focus of 5G-NR, the NR in the unlicensed band, NR-U in release 16 has provisions for standalone LTE operations in the unlicensed band as envisioned by eMTC-U.

C. LWA

LWA is perhaps the most widely studied approach towards the co-existence of LTE and WiFi to enhance the cellular user experience. In fact substantial 3GPP standardization activities have taken place in release 13 [41] and 14 [4]. A new Xw logical interface between eNB and WT [52] is suggested. A new data transport procedure over the Xw interference [53] is proposed. The PDCP layer function is defined for an LWA bearer [54], and finally, a new sublayer the LWA adaption protocol (LWAAP) layer that sits between the PDCP and the RLC [55] is specified. The 3GPP is continually updating the standards in the releaser later.

In LWA the PDCP PDU is offloaded to the WiFi LLC. The LTE-eNB and WiFi-AP can either be collocated or non-collocated. When collocated, both the LTE-eNB and the WiFi-AP are in the same device. By contrast, when non-collocated, the eNB and AP are connected through the Xw logical-interface [56].

D. LWIP

Unlike LWA, LWIP operates above the PDCP layer. LWIP works by encapsulating the IP data in the IPsec tunnel and is directly presented to the WiFi STA, using the legacy WiFi architecture. A separate specification by the 3GPP describes the data encapsulation in LWIP [57]. LWIP works on user-plane both in the uplink and downlink direction.

We summarize the LTE-WiFi co-existence schemes in Table 1.

III. SYSTEM MODEL

We keep our system model generic. We assume N different heterogeneous paths that a UE is connected to the NG-eNB [58]. These heterogeneous networks can either be different enodeBs of the same radio access technology (RATS) or different RATS.

TABLE 1. Summary of LTE-WiFi co-existence Schemes.

Scheme	Coexistence mechanism	Features	Challenges	Proposed by	Proposed first
LTE-U	Unlicensed band without LBT	Easy to implement	Interference and poor spectral efficiency	LTE-U Forum, March 2014	Mar-14
LAA	LTE transmission Unlicensed band with LBT	Interference can be controlled. Significant throughput rise	Scalability to multiple base stations	3GPP	Nov-14
MulteFire	Standalone LTE unlicensed transmission using WiFi AP	Cheaper than licensed operations	Density and traffic of unlicensed band increases	MulteFire Alliance	Jan-17
LWA	PDCP PDU offloading either collocated or non-collocated through Xw logical interface	Uses resources both at eNB and at WiFi AP	Efficient use of resource and latency managenment	3GPP	Jan-16
LWIP	IP PDUs offloading through IPsec Tunnel	No changes in the UE as aggeregation is above PDCP, works both in UL and DL	Addition of LWIP node after IP layer	3GPP	Apr-16

A. OVERVIEW

Consider a piece of user equipment (UE), that connects to N heterogeneous networks (like LTE, WiFi, 5GNR). There is one network, say $i = 1$, that is the primary network of the UE.[1] The other networks, $i = 2, \ldots, N$, are called the secondary networks. Each of the N networks receives the signals (data) in parallel. The received signals can either be hard-decoded at the physical layer to obtain binary bits or soft decoded to obtain LLRs. The receiver is equipped with sufficient buffer storage so that the data through networks with lesser delay can wait for data from other networks. Typically, the primary connection is assumed to be slower than the secondary networks. We provide an overview of the scheme in Fig. 1. Next, we explain the transmitter and the receiver parts.

B. TRANSMITTER

At the NG-eNB, the arriving IP data undergoes PDCP and RLC operations. The MAC layer of the primary network defines the size of the Transport block. Depending upon this size, the super-MAC groups the RLC PDUs into blocks and assigns a unique sequence number to each block. For the secondary networks, the super-MAC supplies essential information like the addresses of the source and destination, among other things. Note that this sequence number is different from the sequence number assigned at the PDCP and the RLC layers. The sequence numbers assigned here are essentially for synchronized combining of data from multiple connections and not for in-order packet combining.

The different MAC entities now transmit the same data according to the procedures defined in their standards. We now proceed to define a generic system model.

Let the k length bit sequence of the RLC PDU that belong to a single MAC payload at the primary network be denoted as

[1]In 5G non-standalone access, typically a primary eNodeB is called NG-eNB (next-generation eNodeB) [58].

$B = \{b_1, b_2, \ldots, b_k\}$. Multiple copies with the same SN are transmitted through N different MAC entities. The data at the physical layer of MAC entity i is encoded in an n_i length bit sequence $C_{i,B} = \{c_{i,1}, c_{i,2}, \ldots, c_{i,n_i}\}$. This data is modulated using appropriate scheme and is transmitted as signals, whose baseband is represented by X_i, $i \in \{1, 2, \ldots, N\}$. Note that there is an average transmit power constraint at the transmitter $\mathbb{E}[|X_i|^2] \leq P_i$.

C. RECEIVER

The received signal Y_i is as follows,

$$Y_i = G_i X_i + Z_i, \tag{1}$$

where G_i denotes the random multiplicative channel fading inflicting the transmission through network i and Z_i is the associated additive white Gaussian noise. We do not specify the distribution of G_i whereas Z_i is zero mean and unit variance Gaussian Noise. Thus the signal to noise ratio at the receiver conditioned on G_i is $\gamma_{b,i} = |G_i|^2 P_i$.

The receiver then demodulates and decodes the LLRs for each bit $j = \{1, \ldots, k\}$ from each network i. At this point the receiver has two options, either to hard decode the LLRs into bits or keep the LLRs as it is. We adopt both the approaches and compare them. Let the bits decoded be denoted by $\tilde{C}_{i,B} = \{\tilde{c}_{i,1}, \tilde{c}_{i,2}, \ldots, \tilde{c}_{i,n_i}\}$.

The receiver now decodes the bits and does one of the following two, as shown in Fig 1. Along with the decoding the bits, the receiver can now either store the LLRs of the RLC PDUs or discard the LLRs and keep only the channel gain values corresponding to a bit.

The receiver checks all the N paths for an error-free block. If any path declares an error-free block's reception, it reports the sequence number of this block to the primary MAC (PMAC) and the PMAC sends the error-free data to the RLC layer. By contrast, if all blocks run into an error, then
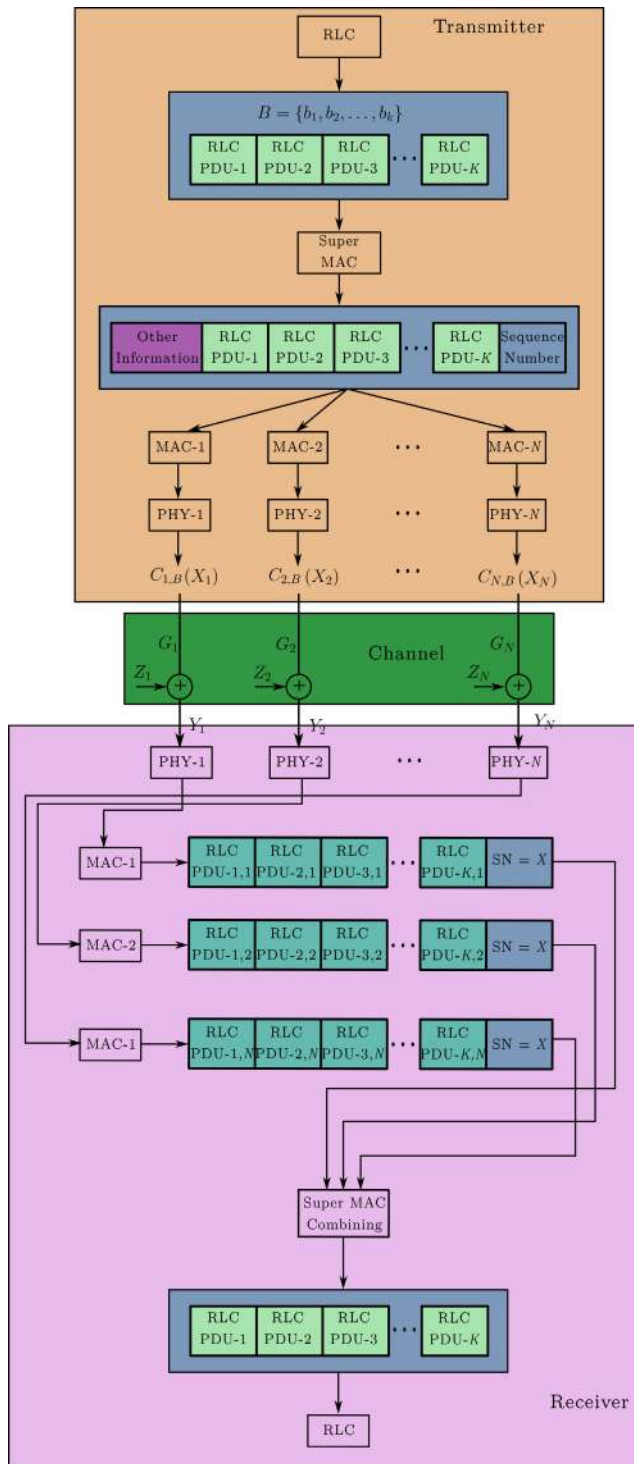
FIGURE 1. The MAC based combining scheme from the NG-eNB PDCP to the UE PDCP.

super-MAC initiates combining. The super-MAC accumulates and synchronises the data using the SN, and combines them according to sequence numbers. This combining can be soft-combining, where the receiver stores and combines the LLRs. The receiver may employ hard combining, where the receiver uses the channel state information along with hard-

decoded bits to combine data. We present details on the two types of combining in sections that follow.

Now, the receiver checks the combined data for errors. If data combining corrects the errors, then the primary network of the UE sends an ACK to the NG-eNB, and the NG-eNB initiates new data transmission. On the other hand, if there is error despite combining, then the primary network of the UE sends a NACK and requests retransmission for the same erroneous block of data.

Remark 1: Although we discuss downlink operations, our cross-layer technique requires data to flow back from super-MAC to the physical layer at the UE, increasing the fixed receiver delay in decoding. However, we show that the technique's reliability ensures lower retransmissions, resulting in low average decoding delay.

We discuss the receiver operations in the event of super-MAC combining.

1) PHYSICAL LAYER OPERATIONS AT THE RECEIVER
The receiver has to perform de-interleaving, de-scrambling and cyclic redundancy check (CRC) at the physical layer. In hard-combining, the receiver performs these operations in the standard fashion. However, in soft-combining (where we keep the LLRs), only de-interleaving is trivial as it requires pre-multiplying LLRs by a permutation matrix. De-scrambling involves modulo two addition of bits, and in our case de-scrambling is performed as explained next.

2) DE-SCRAMBLING OF LLRS AT THE PHYSICAL LAYER
Let us denote the LLR of the $j-$th bit by $LLR(\tilde{c}_{i,j})$ from network $i, j = \{1, \ldots, n_i\}$. The LLRs of the descrambled bits $LLR(c_{i,j})$ is as follows

$$LLR(c_{i,j}) = \begin{cases} LLR(\tilde{c}_{i,j}), & \text{if } s_{i,j} = 1, \\ -LLR(\tilde{c}_{i,j}), & \text{if } s_{i,j} = 0. \end{cases} \quad (2)$$

To see an explanation for the same, the reader can refer to Appendix X. Next we discuss the MAC sub-layer.

3) AT THE MAC AND RLC SUB-LAYER
The MAC sub-layer converts the LLRs of the MAC headers into hard-bits and leaves the MAC payload as LLRs. All the MAC entities report their erroneous payload receptions to the super-MAC. The super-MAC aligns all the erroneous receptions according to the sequence number. Note that since in LTE there are 8 HARQ processes, the super-MAC will also maintain a maximum of 8 MAC payloads. Next, we describe the combining schemes employed by the super-MAC. However, before that, we provide a little background on soft-combining, which will allow us to build our combining scheme.

4) SOFT-COMBINING
Soft-combining (SC) involves combining soft-values (SVS), instead of bits. The receiver assigns higher weights to those bits received with higher SNR. Consequently, SVs can be in

the form of the Log-Likelihood Ratios [59] or can be receiver computed confidence values [60].

Chase combining (CC) and incremental redundancy combining (IRC) use SC in hybrid ARQ procedures [61], [62], where a receiver stores a corrupted (not decodable) packet and soft-combines it with a retransmitted packet arrived. The retransmitted packet may either be an identical copy of the first transmission as in CC or different as in IRC.

The soft-combining approach of combining bits is akin to the maximal ratio combining [63] where instead of bits, different copies of the same (weak) received signals are combined to form a strong signal with optimum SNR. In soft-combining, since we combine SVs of each bit, the idea is to obtain a combined SV that will have the correct sign, i.e. positive for bit 1 and negative for bit 0. Next, we discuss the combining schemes proposed.

IV. COMBINING DATA AT THE SUPER-MAC
At the super-MAC, LLRs corresponding to the RLC PDUs are combined. Since, at the transmitter these bits were $B = \{b_1, b_2, \ldots, b_k\}$, the LLR for bit b_j from path i is denoted as $LLR(b_{i,j})$.

Associated with $LLR(b_{i,j})$ is CSI $H_{i,j}$, where $j = \{1, 2, \ldots, k\}$. Note that $H_{i,j}$ will be derived from G_i. Let N_c be the number of bits that span a coherence interval. If the bits $d_{m,i}$ denote data over a coherence interval, $m = \{1, 2, \ldots, N_c\}$ then for all those $|N_c|$ number of bits, $H_{m,i} = G_i$ which is a constant over the coherence interval. For the sake of simplicity, let us assume that BPSK modulation is employed for all paths. [2] As a consequence the received baseband signal is now,

$$Y_{i,j} = H_{i,j}X_j + Z_{i,j}, \qquad (3)$$

Notice that $X_{i,j}$ is now X_j, that is each path transmits the same value $X_j = 1$ for $b_j = 1$ and $X_j = -1$ for $b_j = 0$. Let $Y_j = \{Y_{1,j}, Y_{2,j} \ldots Y_{N,j}\}$, and $H_j = \{H_{i,j}, H_{2,j} \ldots H_{N,j}\}$. Note that at the receiver Y_j is the received signal and H_j is estimated. We now have the following result

Lemma 1: The optimal soft-combining rule for b_j is calculating the combined Log-Likeihood Ration $LLR(b_j) = 2 \sum_{i=1}^{N} \frac{\Re\{Y_{i,j}H_{i,j}^*\}}{\sigma_i^2}$ and the decoding rule is

$$\hat{b}_j = \begin{cases} 0 & \text{if, } LLR(b_j) < 0 \\ 1 & \text{otherwise.} \end{cases} \qquad (4)$$

Proof: In Appendix E. □

In the case of hard-combining[3], the following test statistic can be employed:

$$L\hat{L}R(b_j) = 2 \sum_{i=1}^{N} |H_{i,j}|^2 (2\hat{b}_{i,j} - 1). \qquad (5)$$

[2]This simplifying assumption makes the analysis for the combining rule tractable. For higher order modulation schemes the analysis is much harder and is beyond the scope of this paper.

[3]Hard-combining becomes necessary when LLRs need to re-created. This happens when coding employed at the transmitter is not systematic.

Here, $\hat{b}_{i,j}$ is the hard-decoded bit estimate on the $i-$th path. Also, since we have lost the LLRs in hard decoding and wish to incorporate the role in combined bit decision making, we estimate the LLR in $L\hat{L}R(b_j)$ for the $j-$th bit. The decision rule will now be similar to the above rule for soft combining and is arrived at as follows.

The estimate of the baseband BPSK signal $\hat{X}_{i,j} = 2\hat{b}_{i,j} - 1$. Now since $Y_{i,j} = H_{i,j}X_{i,j} + Z_{i,j}$, thus one could write, after decoding $\hat{Y}_{i,j} = H_{i,j}\hat{X}_{i,j} = H_{i,j}(2\hat{b}_{i,j} - 1)$. Thus $L\hat{L}R(b_{i,j}) = 2\Re\{\hat{Y}_{i,j}H_{i,j}\} = |H_{i,j}|^2(2\hat{b}_{i,j} - 1)$.

Thus the decoding rule here becomes,

$$\hat{b}_j = \begin{cases} 0 & \text{if, } L\hat{L}R(b_j) < 0 \\ 1 & \text{otherwise.} \end{cases} \qquad (6)$$

We have the following result

Lemma 2: The Hard-combining scheme of (5) has the same probability of error as that of selection combining for $N = 2$.

Proof: In appendix F □

This implies that when hard-decoding is followed by data-combining from two paths then selection combining is optimal. Next we derive the improvement in the block error rate as a result of combining.

V. BLER CALCULATIONS
In this section, we compute the improved probabilities of block error. Let PHY_i, $i = \{1, \ldots, N\}$, denote the $i-$th physical layer. PHY_i transmits a block of length $N_i = N_M + M_i$, where M_i is the total number of bits present in the PHY and MAC headers of i, and N_M is the number of RLC-PDU bits that each MAC layer presents to the super-MAC for combining. Note that N_M is constant across different MACs.

Each of the N physical layer entities, PHY_i will do a CRC check and the initiate combining at the super-MAC. After super-MAC combining the PMAC will do FEC for error correction. If FEC is successful, the super-MAC passes the data to the higher layers else request retransmission. We analyse BLER improvement due to super-MAC combining next.

We consider a block of data at the MAC-i. Let K_i denote the random variable (r.v.) of the number of bit errors in a block at MAC_i, $i = \{1, \ldots, N\}$. Also let t_i be the error correcting capability of the MAC_i. Let the probability of bit error be denoted by p_i. Also, let $\mathscr{E}_i = \{K_i \geq t_i\}$ denote the r.v. modeling the event that PHY_i has a block a error after HARQ (without combining). Then the probability of $\mathscr{E}_i$, denoted by $p_{b,i}$ is given by

$$p_{b,i} = \sum_{k=t_i+1}^{N_M} \binom{N_M}{k} p_i^k (1-p_i)^{N_M-k} \qquad (7)$$

where p_i is the average probability of bit error. The exact expression for p_i depends upon fading distribution and the average SNR $\bar{\gamma}_{b,i} = \mathbb{E}[|H_i|]^2 P_i$. For BPSK signalling the expressions of p_i for well-known distributions are given in Appendix B.

The super-MAC initiates combining when the event $\mathscr{E} = \bigcap_{i=1}^{N} \mathscr{E}_i$ occurs. The super-MAC combines the bits from all the MAC_i's. Post-combining, let the r.v. $\bar{K}_i = K_i - C_i + E_i$ denote the number of errors in the N_M bits at MAC_i, where r.v's C_i and E_i denote the errors corrected and committed in combining, respectively. The super-MAC successfully decodes the data of MAC_i if $\bar{K}_i \leq t_i$. Let $\bar{\mathscr{E}}_i = \{\bar{K}_i \geq t_i + 1\}$. Then a block is in an error when $\bar{\mathscr{E}} = \bigcap_{i=1}^{N} \bigcap_{j=1}^{N} \mathscr{E}_i \bar{\mathscr{E}}_j$ occurs.

Now we look at the r.v.s C_i and E_i. Note that C_i runs over $\{0, 1, \ldots, K_i\}$ while E_i runs over $\{0, 1, \ldots, N_M - K_i\}$. Now let q_i be the probability that an incorrect bit in MAC_i was corrected post combining and let r_i be the probability that a correct bit in MAC_i was erred post combining. For soft combining

$$q(i) = \Pr\left\{ \sum_{i=1}^{N} \frac{\Re\{Y_i H_i^*\}}{\sigma_i^2} > 0 \,\Big|\, \hat{X}_i = -1, X = 1 \right\} p_i \quad (8)$$

$$r(i) = \Pr\left\{ \sum_{i=1}^{N} \frac{\Re\{Y_i H_i^*\}}{\sigma_i^2} > 0 \,\Big|\, \hat{X}_i = -1, X = -1 \right\} (1 - p_i) \quad (9)$$

We can compute this probability for a given fading distribution, but this is a complicated computation. For hard-combining, we derive the expression for this probability in Lemmas 3 and 4 for the cases where the fading is identical Rayleigh distributed and when fading is Rayleigh but with distinct mean values respectively.

Lemma 3: For hard-combining at the super-MAC, when $|H_j|$ are iid Rayleigh random variables over N (or equivalently $|H_j|^2$ are iid exponential), we have

$$q(i) = \sum_{\mathcal{P}_i \in 2^{\mathcal{S}_{-i}}} \left[\int_{x=0}^{\infty} \left(\int_{y=0}^{x} f_E(y, \lambda, |\tilde{\mathcal{P}}_i^c|)) dy \right) \right.$$
$$\left. f_E(x, \lambda, |\mathcal{P}_i|) dy \right] \prod_{j \in \mathcal{P}_i} \prod_{k \in \tilde{\mathcal{P}}_i^c} p_j (1 - p_k) \quad (10)$$

and

$$q(i) = \sum_{\mathcal{P}_i \in 2^{\mathcal{S}_{-i}}} \left[\int_{x=0}^{\infty} \left(\int_{y=0}^{x} f_E(y, \lambda, |\mathcal{P}_i^c|)) dy \right) \right.$$
$$\left. f_E(x, \lambda, |\tilde{\mathcal{P}}_i|) dy \right] \prod_{j \in \tilde{\mathcal{P}}_i} \prod_{k \in \mathcal{P}_i^c} p_j (1 - p_k) \quad (11)$$

Proof: See Appendix C. $\square$

Lemma 4: For hard-combining at the super-MAC, when $|H_j|$ are independent but with different mean valued Rayleigh distributed over N, we have

$$q(i) = \sum_{\mathcal{P}_i \in 2^{\mathcal{S}_{-i}}} \left[\int_{x=0}^{\infty} \left(\int_{y=0}^{x} f_{EM}(y, \boldsymbol{\lambda}_{\tilde{\mathcal{P}}_i^c}, |\tilde{\mathcal{P}}_i^c|)) dy \right) \right.$$
$$\left. f_{EM}(x, \boldsymbol{\lambda}_{\mathcal{P}_i}, |\mathcal{P}_i^c|) dx \right] \prod_{j \in \mathcal{P}_i} \prod_{k \in \mathcal{P}_i^c} p_j (1 - p_k) \quad (12)$$

and

$$r(i) = \sum_{\mathcal{P}_i \in 2^{\mathcal{S}_{-i}}} \left[\int_{x=0}^{\infty} \left(\int_{y=0}^{x} f_{EM}(y, \boldsymbol{\lambda}_{\mathcal{P}_i^c}, |\mathcal{P}_i^c|) dy \right) \right.$$
$$\left. f_{EM}(x, \boldsymbol{\lambda}_{\tilde{\mathcal{P}}_i}, |\tilde{\mathcal{P}}_i|) dx \right] \prod_{j \in \mathcal{P}_i^c} \prod_{k \in \tilde{\mathcal{P}}_i} p_j (1 - p_k) \quad (13)$$

Proof: See Appendix D. $\square$

We then have the next result that characterizes the probability of the event $\bar{\mathscr{E}}_i^c$, the event that super-MAC corrected a block in error.

Lemma 5: Denote $G_N(k; p) = \binom{N}{k} p^k (1 - p)^{N-k}$. The probability of $\bar{\mathscr{E}}_i^c$ is then

$$q_{b_i} = Pr\{K_i - C_i + E_i \leq t_i\}$$
$$= \sum_{k_i = t_i + 1}^{N_m} \sum_{e_i = 0}^{l_i} \sum_{c_i = m_i}^{k_i} G_{k_i}(c_i; q_i) G_{N_M - k_i}(e_i; r_i) G_{N_M}(k_i; p_i) \quad (14)$$

where $l_i = \min(t_i, N_M - k_i)$ and $m_i = k_i - t_i + e_i$.

Proof: In Appendix G. $\square$

Notice that the minimum number of errors that need to be corrected by the super-MAC to declare an error-free block at MAC_i is $C_i = K_i + E_i - t_i+$. However, this number can be at-most K_i and thus, if $E_i \geq t_i$, then the block cannot be corrected. On the other hand if $C_i - E_i > K_i - t_i$ then the block is corrected. Thus finally the BLER is given by

$$\tilde{p}_b = \prod_{i=1}^{n} p_{b,i} (1 - q_{b,i}) \quad (15)$$

Clearly $\tilde{p}_b < \prod_{i=1}^{n} p_{b,i}$. That is if we employ a simple selection rule to approve the data that has successfully decoded the data, then the BLER would be $\prod_{i=1}^{n} p_{b,i} p_{b,i}$. Now due to super-MAC, the BLER is improved by a factor $\prod_{i=1}^{n} (1 - q_{b,i})$.

In the next section, we provide the latency analysis and show that the system's average latency also improves due to improved BLER.

VI. LATENCY ANALYSIS

The 3GPP [64] defines latency as the time taken for a PDCP SDU to reach from the transmitter to the receiver.

Note that the total user-plane latency comprises of two components [65], (i) one-way latency due to the transmitter and receiver processing delays and the transmission time interval, and (ii) the average round trip time, that depends upon the block error rate that dictates the random number of round trips.

Since the data is combined at the super-MAC and then sent down to the lower layers, the fixed one-way latency increases, however, the average delay in the system is expected to decrease because combining the data reduces the block error rate and with it the average number of round trips.

Let T_t and T_r denote the fixed transmitter and receiver processing delays in the standalone system. Also, let T_{TTI} and T_{RTT} denote the transmission time interval and round trip

time, respectively. Then the average latency in the standalone scenario for FDD based communications is given by

$$L_s = T_t + T_r + T_{TTI} + p_{b_1} T_{RTT}, \qquad (16)$$

where we have assumed, without loss of generality, that $i = 1$, represents the primary network. Although the latencies of the secondary networks are lesser than the primary network, the PMAC will dictate the latency value because the acknowledgements are sent through the primary network.

There is an additional delay component at the super-MAC and the re-performing of the CRC checks for the combined system. We denote this collectively by T_s. The latency for the combined system will then be

$$L_c = T_t + T_r + T_{TTI} + \prod_{i=1}^{N} p_{b_i} T_s + p_b T_{RTT} \qquad (17)$$

We scale the delay component at super-MAC by $\prod_{i=1}^{N} p_{s_i}$ because the combining scheme is employed only when there is a block error in all MAC entities. Also per block, the combining takes only kN real additions in case of soft combining and $2kN$ real additions and kN real multiplications in hard combining. If N is high, then $\prod_{i=1}^{N} p_{b_i} \rightarrow 0$, while if $N = 2$, then the number of real additions and multiplications are substantially low. Thus, the computational complexity of these operations is negligible. Secondly, the CRC check process forms a small component of T_r which involves decoding, demodulating, deinterleaving and descrambling along with other processes till the super-MAC and this, coupled with the fact that the delay occurs with a small probability, the overall contribution can be safely neglected. Hence the average latency with combining can be approximated as

$$L_c \approx T_t + T_r + T_{TTI} + p_b T_{RTT} \qquad (18)$$

However, we also look at an upper bound to latency, where we assume that the receiver processing delay is at most twice that of the standalone system when a block is in error before combining. We do make a small assumption that no detection of signals in the second traversing offsets the delay in data combining.

The combining of LLRs incurs N real-additions per bit. Assuming that the block of RLC PDUs is k bits, we have kN such additions. The processing delays of modern DSPs are minimal. Even if we consider the 5G NR fixed receiver processing delay of a fraction of a millisecond, the processing delay T_p for N additions is significantly smaller than T_r, that is $T_p \ll T_r$. Moreover, in the combining scheme, the fixed receiver operations such as detecting, deinterleaving and descrambling are not performed. Hence, we can safely assume that the fixed receiver processing delay in combining is less than $2T_r$. Nevertheless, we assume the upper bound and show that combining still achieves lesser latency in many interest cases.

Hence, the latency in the combining scheme, is

$$L_c = (1 - \prod_{i=1}^{N} p_{b_i})(T_t + T_r + T_{TTI}) \qquad (19)$$

$$+ \prod_{i=1}^{N} p_{b_i}(T_t + 2T_r + T_{TTI})$$
$$+ p_b T_{RTT}$$
$$= T_t + T_{TTI} + (1 + \prod_{i=1}^{N} p_{b_i})T_r + p_b T_{RTT} \qquad (20)$$

For $L_c < L_s$, a sufficient condition is,

$$\prod_{i=1}^{N} p_{b_i})T_r + p_b T_{RTT} < p_{b_1} T_{RTT} \qquad (21)$$

Since $p_b < \prod_{i=1}^{N} p_{b_i}$ from (15), then a sufficient condition for $L_c < L_s$ is

$$\prod_{i=2}^{N} p_{b_i} < \frac{T_{RTT}}{T_r + T_{RTT}} \qquad (22)$$

Typically, $T_{RTT} \approx 5T_r$ [66] (or $8T_{TTI}$ due to 8 simultaneous HARQ processes), which implies that the average latency improves through data combining if $\prod_{i=2}^{N} p_{b,i} < \frac{5}{6}$, which is certainly true in most cases of practical interest. In sections that follow, we will see how the combining scheme will help in reducing latency.

VII. COMPATIBLE DATA RATES AND POSSIBLE SCENARIOS

The average data rates achievable through the secondary MAC (SMAC) entities must be more than the those achievable through the PMAC. For example, if WiFi has to assist NR through the super-MAC, then WiFi must be capable of bearing the NR MAC-payload with an average latency lower than NR and such that the super-MAC achieves target BLER after combining. In such a case, we say that SMAC (WiFi in this case) is compatible with the PMAC. In most cases, we can ensure that the SMAC is compatible with PMAC and SMAC by tuning various SMAC parameters that affect the data rates. These parameters include, modulation and coding schemes, number of resource units and MIMO capability. When multiple SMACs are involved, we require that all the individual SMACs be compatible with the PMAC. When all SMACs are compatible with PMAC, then we say that the different paths have compatible data rates.

Note that applications that perform data offloading do not require the SMAC to be compatible with PMAC in the sense we have defined above.

In the next section, using an example of 4G-LTE as PMAC, and 5G-NR and IEEE 802.11ac WiFi as SMACS, we show a wide range of compatible rates exists that allow WiFi to work with LTE and 5G-NR also to work with LTE.

A. POSSIBLE SCENARIOS
Since we have assumed a generic model, N can be arbitrary. However, in practice, multi-connectivity has not yet been realized for $N > 2$. The 3GPP has defined new interfaces. These interfaces can establish a multi-RAT and multi-connectivity as shown in Fig. 2, which
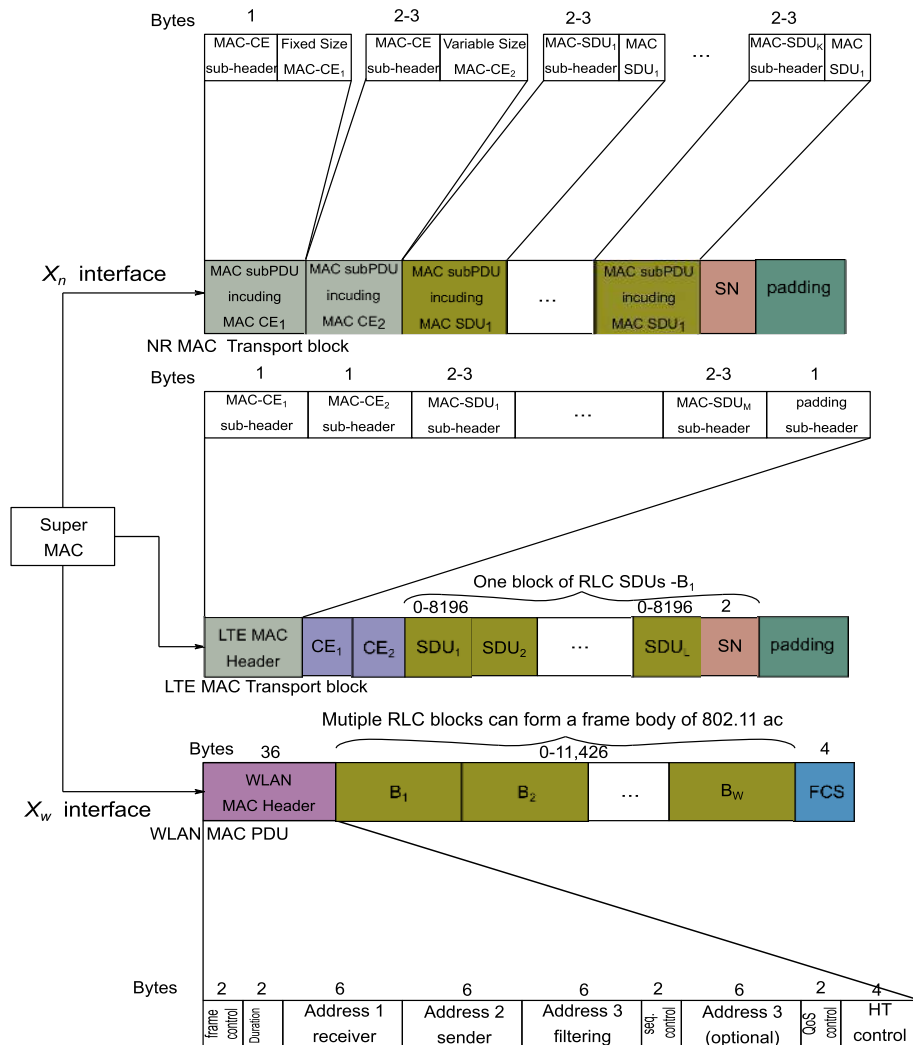
FIGURE 2. An example of a Multi-RAT multi-connectivity scenario.

depicts the multi-connectivity of primary NG-eNB, a standard 4G-eNodeB, a 5G-gNB and a WiFi AP. Here NG-eNB is the master which hosts the super-MAC and passes the RLC PDU to the (i) eNodeB through the X2 interface, (ii) 5G-gNB through the Xn interface and (iii) to the WiFi AP through the Xw interface.

The super-MAC achieves synchronization by marking a group of RLC PDUs with SN. It is essential to ensure that all the SMACs have latency lesser than that of NG-eNB direct path for latency-sensitive applications. However, for bandwidth-hungry applications that are latency-tolerant, the multi-connected system can enhance throughput while ensuring reliability. We simulate an example at the intersection of dual-RAT and dual-connectivity for reliability enhancement, through a super-MAC based combining of 4G-LTE and WiFi (802.11ac) followed by the LTE-NR and NR-WiFi scenarios. This simulation-based study will demonstrate the performance improvement achieved by the combining scheme in terms of BLER and throughput. In many regimes of interest, combining also improves the latency along with BLER and throughput.

VIII. COMBINING SCENARIOS

We consider two scenarios for further study. In the first scenario, we consider LTE-WiFi and analyze the BLER, Throughput and Latency performance for sub-scenarios spanning different modulation and coding schemes. This simulation demonstrates the performance improvement as a result of the two combining schemes. In the second scenario, we consider three sub-scenarios: LTE-NR, NR-WiFi and LTE-WiFi for BLER and throughput. The second scenario compares the

performances of both our schemes to that of the PDCP based duplication scheme as proposed in [33].

We first take an example of LTE assisted by WiFi. We depict the interaction of the super-MAC and MACs of both LTE, WiFi and NR in Fig. 3.

From the figure, we see that a group of RLC PDUs form a block. The block size can be significant to make a long transport block. However, we assume that the at-least one block fits the WiFi MAC frame body. Selecting compatible rates ensures this. We examine the peak rates achievable for LTE, WiFi and NR, which allow us to characterize the rates of WiFi and NR that can be compatible for a given LTE peak rate, and also the rates of WiFi that can be compatible for a given NR peak rate.

A. LTE PEAK DATA RATE

As per 3GPP release 12 [16], for LTE, each frame is of 10 ms duration and is divided into 10 sub-frames each of $T_{s,l} = 1$ ms duration. Each subframe consists of $T_s = 2$ time slots. A UE is assigned with at least one physical resource block (PRB). A PRB consists of $N_c = 12$ subcarriers, each of which has a fixed bandwidth of $\Delta F_L = 15$ kHz. Also each PRB consists of $N_s = 7$ OFDM symbols when normal cyclic-prefix is used and $N_s = 6$, when extended cyclic-prefix is used. Each OFDM symbol consists of b_L bits for $M - QAM$, where $b = \log_2 M$. Let B_L be the available bandwidth to a UE. Corresponding to this bandwidth, let N_{prb} be the number of PRBs that can be allocated to the UE. Let the code rate be C_l. For MIMO systems let the multiplexing gain be G_l. We then have r_{LTE}, that is the peak data rate available to a UE as follows

$$r_{LTE} = C_l G_l \frac{N_{prb} N_c N_s T_s b_L}{T_{s,l}}$$

As an example rate calculation, suppose a total bandwidth of $B = 10$ MHz, is available to a UE. This corresponds to $N_{prb} = 50$. Assuming, $C_l = \frac{3}{4}$ transmission, 4×4 MIMO with normal cyclic-prefix and $16 - QAM$, we have the rate

$$r_{LTE} = \frac{2s \times 50 \times 12 \times 7 \times 2 \times 4}{10^{-3}}$$
$$= 96.13 \text{Mbps}$$

The reader can refer table 7.1.7.1-1 of [16] for more details.

B. WiFi PEAK DATA RATE

As per [67], in the 802.11ac, for bandwidth B_w there is a fixed number of subcarriers N_w each having sub-carrier spacing of $\Delta F_w = 312.5$ kHz. Thus the symbol duration is $3.2\mu s$. A short guard interval lasts 400 ns while long lasts 800 ns. The symbol duration is $T_{s,w} = 3.6\mu s$ for short-guard interval and $4\mu s$ for long-guard interval. For $M - QAM$ modulation, with coding rate C_w and multiplexing gain G_w, we have the peak data rate for bandwidth B_w

$$r_{WiFi} = C_w G_w \frac{N_w b}{T_{s,w}}.$$

FIGURE 3. Super-MAC passes information to all the MACs, that is LTE, NR and WiFi MACs. The WiFi and NR MACs need address for source and destination, which is supplied by super-MAC.

As an example, for $B_w = 20$ MHz, $N_w = 56$. If 16-QAM is used with a short guard interval with $C_w = 3/4$ and $G_w = 4$, we have

$$r_{WiFi} = \frac{3 \times 56 \times 4 \times 10^6}{3.6}$$
$$= 178\text{Mbps}$$

Thus there are scenarios where the achievable rates in WiFi are more than that of the LTE. Similarly, there are many more achievable data rates for WiFi compatible with the LTE rate of 96.13 Mbps. However, as the LTE rate increases, the possible WiFi rates compatible become smaller. An important point to note is that we are interested in scenarios where LTE performance is poor and will typically, have low data rates. Using different modulation and coding schemes and choosing an appropriate MIMO size, one can achieve compatible rates.

C. 5G-NR PEAK DATA RATE
As per [68], the maximum data rate computed for a given number of aggregated carriers in a band or band combination is as follows.

$$r_{NR} = \sum_{j=1}^{J} \left(v_L^{(j)} Q_m^{(j)} f^{(j)} R_m \frac{N_{PRB}^{BW(j),\mu} 12}{T_s^{\mu}} \left(1 - OH^{(j)} \right) \right)$$

wherein J is the number of aggregated component carriers (CC) in a band or band combination, $R_{max} = 948/1024$ (for LDCP codes). For the j-th CC, $v_L^{(j)}$ is the maximum number of supported layers or in other words, the number of MIMO data-streams supported. Also, $Q_m^{(j)}$ is the maximum supported modulation order. Also, $f^{(j)}$ is the scaling factor and can take the values 1, 0.8, 0.75, and 0.4. The scaling factor incorporates the relationship between the maximum number of layers and the band combination's maximum modulation order. If the maximum number of layers and the maximum number of modulation orders are per band and per band combination, the scaling factor becomes unnecessary. For the j-th CC, $v_L^{(j)}$ is the maximum number of supported layers or in other words, the number of MIMO data-streams supported. Also, $Q_m^{(j)}$ is the maximum supported modulation order. μ

TABLE 2. Simulation Scenario - 1 parameters.

MAC parameters		LTE		WiFi	
Access Mode		FDD		CSMA/CA	
Transmission		Downlink		Downlink	
Fading Model		Rayleigh		Rayleigh	
Number of frames		50		500 (packets)	
TTI		1 ms		1 ms	
Frame duration		10 ms		1 ms	
Bandwidth		20 MHz		20 MHz	
Physical parameters		sub-scenario 1		sub-scenario 2		sub-Scenario 3	
	LTE	WiFi	LTE	WiFi	LTE	WiFi
MCS	3	0	8	1	12	2
Peak data rate (Mbps)	7.1	6.5	17.5	14.4	28.42	21.7
Buffer size (Mb)	8.5	8.5	15	15	30	30
SNR (dB)	5, 6, 6.5	7.8, 7.9, 8.0	10, 10.5, 11	11.3 11.4, 11.5	20, 22.5, 23.5	16.8, 17, 17.2
Transport block size (bits)	7992	7992	15264	15264	28336	28336
Simulation time (ms)	4500		4500		4500	

TABLE 3. Simulation Scenario-2 parameters.

MAC parameters		5G		LTE		WiFi	
Access Mode		FDD		FDD		CSMA/CA	
Transmission		Downlink		Downlink		Downlink	
Fading Model		Rayleigh		Rayleigh		Rayleigh	
Number of frames		25		50		500 (packets)	
TTI		1 ms		1 ms		1 ms	
Frame duration		10 ms		10 ms		1 ms	
Bandwidth		20 MHz		20 MHz		40 MHz	
Physical parameters		sub-scenario 1		sub-scenario 2		sub-scenario 3	
	5G	LTE	5G	WiFi	LTE	WiFi
MCS	23	12	23	1	12	1
Peak data rate (Mbps)	30	27.5	30	30	27.5	30
Buffer size (Mb)	30	30	30	30	30	30
SNR (dB)	10, 11, 12	10, 12, 14	10, 11, 12	11, 11.5, 12	10, 12, 14	11, 11.5, 12
Transport block size (bits)	30216	30216	30216	30216	30576	30576
Simulation time (ms)	4500		4500		4500	

is the numerology (as defined in [69]), T_s^{μ} is the average OFDM symbol duration in a subframe for numerology μ with normal cyclic prefix. $N_{PRB}^{BW(j),\mu}$ is the maximum number of resource blocks that can be allocated in bandwidth $BW^{(j)}$ with numerology μ, $BW^{(j)}$ is the UE supported maximum bandwidth in the given band or band combination. As an example, for a 20MHz bandwidth with $\mu = 1$ corresponding to a sub-carrier spacing of 30 KHz, $N_{PRB} = 51$. For $J = 1$, $v_L = 1$, $Q_m = 4$, 14% overhead and unit scaling factor, the maximum data rate is 109.15 Mbps which is clearly compatible with an LTE rate of 96 Mbps.

Next, we perform simulation for the LTE-WiFi based dual-connected system in detail. Also, we simulate the scenarios of LTE-NR and NR-WiFi.

IX. SIMULATIONS

We perform simulations for the two scenarios as follows:

- Scenario 1 compares the performance of LTE standalone with that of WiFi assisted LTE, where LTE is the primary network. The performance indicators are BLER, Throughput and Latency. Simulation parameters for this scenario are listed in Table 2. We choose the SNRs such that three different MCSs with compatible rates each are selected. The MCSs for standalone LTE are the MCS-3,8 and 12, while their compatible counterparts in WiFi are MCS-0,1 and 2, respectively. One can certainly select higher order MCS for WiFi; however, this will offer better performance at the cost of more resources.

- Scenario 2 compares the performance of the PDCP based duplication (PDCP) scheme [33] with that of the super-MAC based schemes proposed in this paper. Simulation parameters for this scenario are listed in Table 3. The performance indicators are BLER and Throughout. We consider three sub-scenarios as follows. Firstly LTE-NR with LTE as the primary network, then

NR-WiFi with NR as the primary network, and finally a version of LTE-WiFi with LTE as the primary network is considered. Note that the MCSs chosen are such that all these three combining strategies have compatible rates.

Since the key performance indices (KPI) of interest are the BLER, throughput, and Latency (only for Scenario 1) we first define each of the terms as per 3GPP.

Definition 1 (BLER): The BLER is defined as the fraction of code-blocks that have failed the CRC after all error correction schemes.

The physical layer segments the MAC-PDUs or the transport blocks into appropriate size code-blocks and appends each code-block with CRC bits.

Definition 2 (Throughput): The measured UE Application Layer Throughput is defined as the number of useful user data bits per unit of time delivered by the network from the source endpoint to the destination endpoint, excluding protocol overhead (headers) and retransmitted data packets. Although this refers to the application layer throughput, we can extend this definition to the lower layers, like the PDCP, where the volume of data measured is successfully transmitted to the same layer at the receiver, excluding the lower layer headers.

Definition 3 (Latency): The 3GPP defines Latency as the time taken for a PDCP SDU to reach from the transmitter to the receiver (UE).

Note that this definition applies to 3GPP networks. Similarly, one may define the latency of WiFi to be the delay encountered in MAC-PDUs to reach from the transmitter (AP) to the receiver (STA).

A. RESULTS AND ANALYSIS

We first discuss the results and present a detailed analysis of Scenario-1. A discussion and analysis of Scenario-2 follow this.

B. SCENARIO-1

The Table 4 summarizes the standalone LTE's BLER and throughput performances for the three different MCS scenarios. When the received SNR increases beyond a certain level, the UE notifies the enodeB, which then moves to an MCS, offering better throughput while staying below a certain BLER level. For example, from the Table, we can conclude that when the SNR reaches 10 dB and above, the MCS can now change to MCS-8, which offers higher throughput while maintaining the BLER around 0.3. Certainly, this BLER is not desirable; however, we will show that employing the combining scheme the BLER will reduce to desirable values of near 0.1. Next we summaries the result for BLER in the combined scheme both with soft-combining (SC) and hard-combining (HC) in Table 5 and plot it in Fig. 4. Two observations are immediate. Firstly, the SC-based scheme is superior to the HC-based scheme. Secondly, both schemes offer superior BLER to that obtained by the standalone system. This is better demonstrated in Fig. 5, which plots the BLER against

TABLE 4. BLER, Latency (in ms) and Throughput (in Mbps) for the standalone LTE.

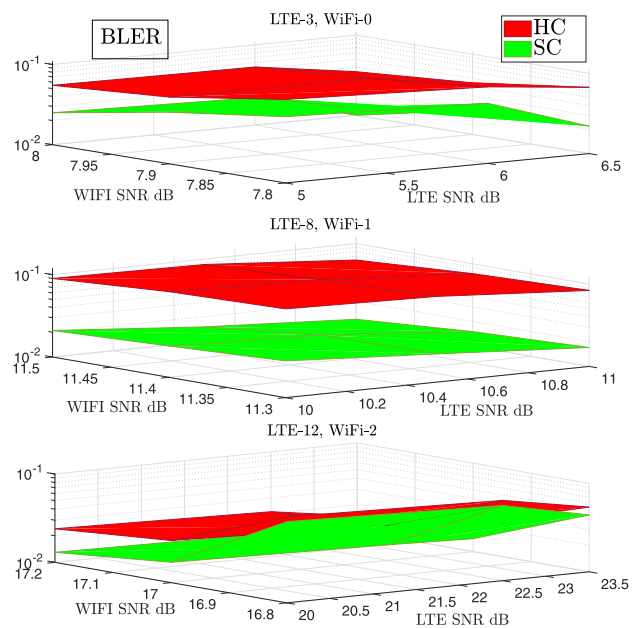| MCS	SNR	BLER	T/put	Latency
MCS-3	5	0.331	2.406	6.65
	6	0.22	2.805	5.76
	6.5	0.176	2.965	5.41
MCS-8	10	0.364	4.366	6.91
	10.5	0.329	4.61	6.63
	11	0.276	4.976	6.21
MCS-12	20	0.336	9.066	6.69
	22.5	0.129	11.88	5.03
	23.5	0.091	12.4	4.73

FIGURE 4. The BLER plot for the combined system in Scenario 1 as per simulation parameters listed in Table 2.

a range of LTE SNRs. Notice that the BLER has a sawtooth-like plot, which results from an MCS change with SNR. Since the transmitter now uses a higher-order modulation, the throughput increases, however, the average bit-error-rate increases leading to a higher BLER. We have selected parameters to achieve a target BLER or around 10%. Notice from the figure that without using WiFi, the standalone LTE suffers significantly high BLER when compared to where WiFi is employed.

Another important observation is that SC and HC's performance gap reduces as the SNR increases in a particular MCS, which implies that HC can be used instead of SC in such regimes and when memory requirements to store soft-bits are stringent.

We now demonstrate the latency reduction due to a decrease in BLER. The average latency for WiFi (802.11 ac at the 5GHz bands) is lesser than that of the 4G LTE but higher than 5G NR URLLC applications. Hence, WiFi can assist 4G LTE and 5G NR emBB applications but not the URLLC
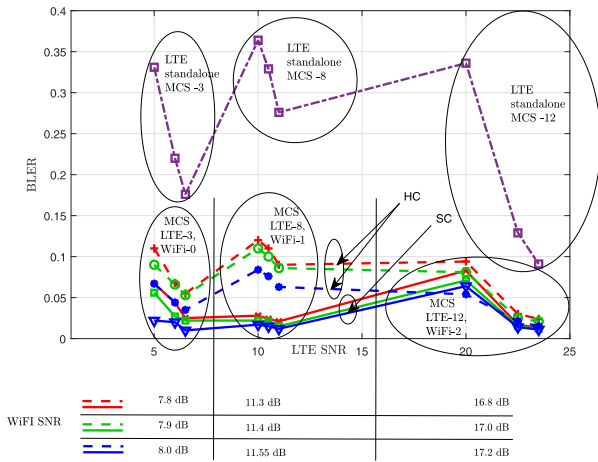
FIGURE 5. A two-dimensional plot shows the sawtooth nature of the BLER curve. The sawtooth appearance is because the MCS changes when SNR moves beyond a certain point.

TABLE 5. BLER for the combined LTE-WiFi system.

W, 0 / L, 3	7.8	7.9	8.0
	SC, HC	SC,HC	SC, HC
5	0.067, 0.11	0.056, 0.09	0.022, 0.067
6	0.044, 0.068	0.027, 0.066	0.020, 0.044
6.5	0.025, 0.055	0.022, 0.053	0.010, 0.035
W, 1 / L, 8	11.3	11.4	11.55
10	0.028,0.12	0.022,0.11	0.017,0.084
10.5	0.024,0.11	0.021,0.1	0.015,0.076
11	0.021,0.09	0.015,0.086	0.012,0.063
W, 2 / L, 12	16.8	17	17.2
20	0.083,0.094	0.071,0.081	0.064,0.054
22.5	0.017,0.03	0.015,0.025	0.014,0.021
23.5	0.013,0.024	0.012,0.021	0.011,0.015

TABLE 6. Latency in milliseconds for the combined LTE-WiFi system (Upper bound).

W, 0 / L, 3	7.8	7.9	8.0
	SC, HC	SC,HC	SC, HC
5	4.7, 5.04	4.58, 4.86	4.28, 4.64
6	4.45, 4.65	4.31, 4.63	4.23, 4.42
6.5	4.2, 4.52	4.26, 4.5	4.13, 4.33
W, 1 / L, 8	11.3	11.4	11.55
10	4.4, 5.14	4.34, 5.05	4.26, 4.8
10.5	4.36, 5.04	4.32, 4.95	4.23, 4.72
11	4.30, 4.86	4.25, 4.82	4.19, 4.6
W, 2 / L, 12	16.8	17	17.2
20	4.81, 4.89	4.69, 4.77	4.59, 4.51
22.5	4.18, 4.29	4.16, 4.24	4.14, 4.2
23.5	4.14, 4.23	4.13, 4.2	4.11, 4.14

application in 5G. We present the latency numbers in Table 6. An important observation from the latency table is that we achieve latency gains by combining when the SNR is low for a given MCS. The low SNR leads to higher standalone BLER
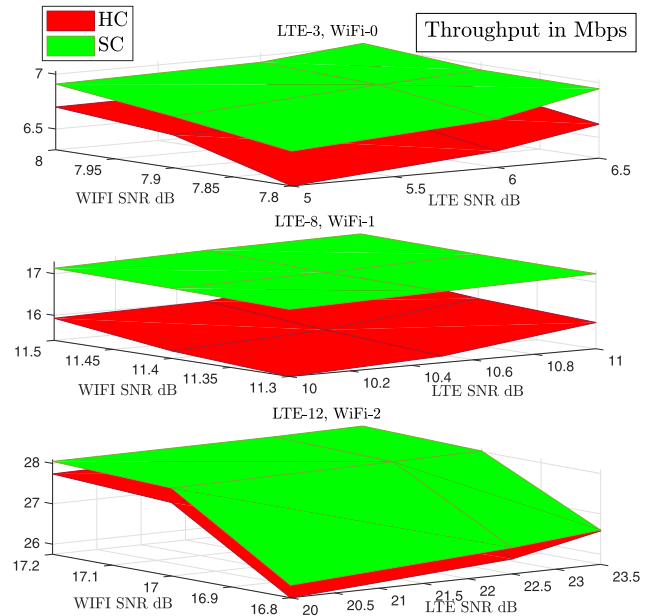
FIGURE 6. Throughput (in Mbps) plot of the combined scheme for Scenario 1 as per the simulation parameters listed in Table 2.
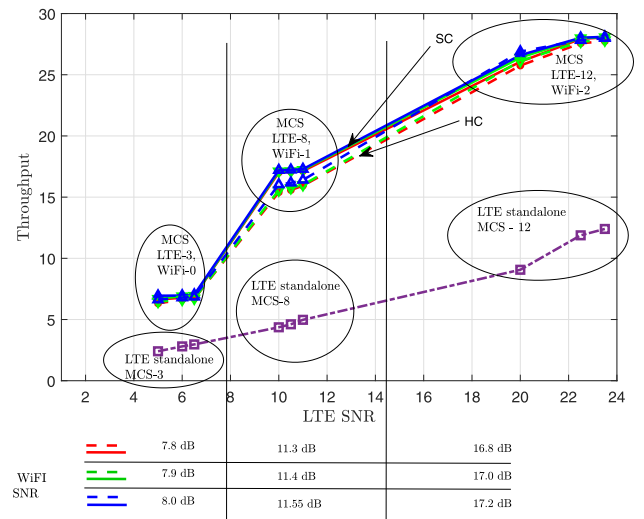
FIGURE 7. A two-dimensional Throughput curve. Contrast this with the sawtooth appearance of the BLER.

and hence combining helps reduce BLER significantly, thus also causing latency to reduce.

Throughput for the combined system is summarized in Table 7 and plotted in Fig 7. The throughput of the combined scheme is substantially higher than that of the standalone system. The throughput increase due to combining over the standalone LTE is relatively more at lower SNRs. Hence, even if a user is at the cell boundary where the signal is weak, the achievable throughput is substantial.

1) RELATIONSHIP BETWEEN THROUGHPUT AND BLER
When all the other parameters are fixed the throughput is directly proportional to $1-$BLER, or Throughput $= c(1 - $ BLER), where c depends upon the modulation and coding

TABLE 7. Throughput (in Mbps) for the combined LTE-WiFi system.

W, 0 / L, 3	7.8	7.9	8.0
	SC, HC	SC,HC	SC, HC
5	6.627, 6.319	6.699, 6.461	6.943,6.624
6	6.786, 6.617	6.906, 6.631	6.958,6.788
6.5	6.919, 6.71	6.942, 6.724	7.029,6.852
W, 1 / L, 8	11.3	11.4	11.55
10	17.01,15.4	17.11, 15.56	17.203,16.03
10.5	17.08,15.58	17.13,15.75	17.23,16.17
11	17.13,15.93	17.23,16.0	17.29,16.4
W, 2 / L, 12	16.8	17	17.2
20	26.06, 25.75	26.4, 26.12	26.6,26.89
22.5	27.93, 27.57	27.99, 27.71	28.02, 27.82
23.5	28.05,27.74	28.07,27.82	28.10,27.99

TABLE 8. BLER, and Throughput (in Mbps) for the standalone NR and LTE as per Simulation parameters listed in Table 3.

MCS	SNR	BLER	Throughput
5G-MCS-23	10	0.512	13.42
	11	0.482	14.24
	12	0.234	21.06
4G-MCS-12	10	0.431	15.65
	12	0.213	21.64
	14	0.043	26.35

TABLE 9. BLER for the combined 5G-LTE-WiFi systems. S1={(5G,23),(4G,12)}, S2={(5G,23),(W,1)}, S3={(L,12),(W,1)}. The column SNRs are of the first network. So for S1, the column SNRs are of (5G,23) and row SNRs are of (4G,12). Similar convention for S2 and S3.

S1	10	12	14
	SC,HC,PDCP	SC,HC,PDCP	SC,HC,PDCP
10	0.094,0.221,0.270	0.053,0.109,0.131	0.015,0.022,0.065
11	0.09,0.207,0.251	0.05,0.102,0.123	0.010,0.020,0.052
12	0.051,0.10,0.23	0.02,0.049,0.058	0.007,0.012,0.05
S2	11	11.5	12
10	0.082,0.161,0.2	0.05,0.102,0.152	0.03,0.052,0.11
11	0.074,0.153,0.19	0.042,0.096,0.141	0.024,0.049,0.09
12	0.032,0.05,0.1	0.021,0.046,0.093	0.015,0.023,0.075
S3	11	11.5	12
10	0.062,0.138,0.181	0.051,0.086,0.142	0.022,0.043,0.092
12	0.033,0.067,0.124	0.035,0.042,0.112	0.014,0.021,0.054
14	0.006,0.013,0.06	0.004,0.008,0.013	0.002,0.004,0.009

FIGURE 8. BLER comparison our combining schemes in scenario-2 with the PDCP based duplication. All three sub-scenarios are plotted here.

TABLE 10. Throughput for the combined systems (in Mbps). S1={(5G,23),(4G,12)}, S2={(5G,23),(W,1)}, S3={(L,12),(W,1)}. The column SNRs are of the first network. So for S1, the column SNRs are of (5G,23) and row SNRs are of (4G,12). Similar convention for S2 and S3.

S1	SC, HC, PDCP	SC, HC, PDCP	SC, HC, PDCP
	10	12	14
10	24.9, 21.4, 20.1	26, 24.5, 23.9	27.8, 26.9, 25.7
11	25, 21.8, 20.6	26.1, 24.7, 24.1	27.2, 27, 26.1
12	26.1, 24.8, 21.2	27, 26.2, 25.9	27.3, 27.2, 26.1
S2	11	11.5	12
10	25.2, 23, 22	26.1, 24.7, 23.2	26.7, 26.1, 24.5
11	25.5, 23.3, 22.3	26.3, 24.9, 23.6	26.8, 26.2, 25
12	26.6, 26.1, 24.8	26.9, 26.2, 24.9	27.1, 26.9, 25.4
S3	11	11.5	12
10	25.8, 23.7, 22.5	26.1, 25.1, 23.6	26.9, 26.3, 25
12	26.6, 25.7, 24.1	26.5, 26.3, 24.4	27.1, 27, 26
14	27.3, 27.1, 25.9	27.4, 27.3, 27.1	27.4, 27.4, 27.2

scheme and bandwidth. The modulation and coding scheme defines the code rate which is essentially specifies the fraction of informatio bits in the total number of bits after coding. Hence, when the MCS and bandwidth are fixed, then throughput will increase when BLER decreases. However, when the MCS changes to a higher index the throughput will increase as the code rate or bandwidth or both increase. However, the BLER may increase in such a case. We can observe this behaviour when Figs. 5 and 7 are viewed together. In our
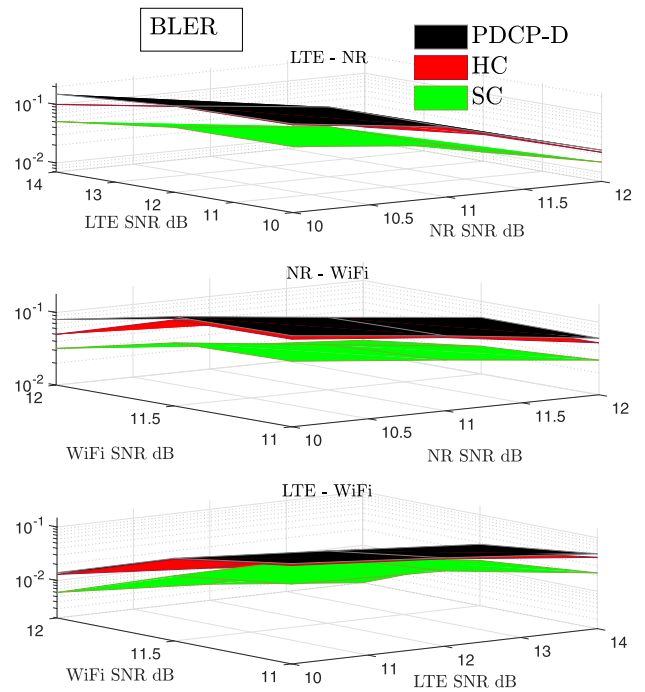
simulations we have maintained the BLER values to around 10% after combining.

C. SCENARIO - 2

The Table 8 shows the BLER and Throughput for the standalone NR and LTE scenarios.

Note that since we wish to show the benefits of combining, we choose the standalone BLER to be high. We will see that all the three sub-scenarios of Scenario-2 reduce the BLER.

Table 8 summarizes the BLER improvement achieved through combining. Firstly, both the combining schemes outperform the PDCP based duplication scheme. In the PDCP
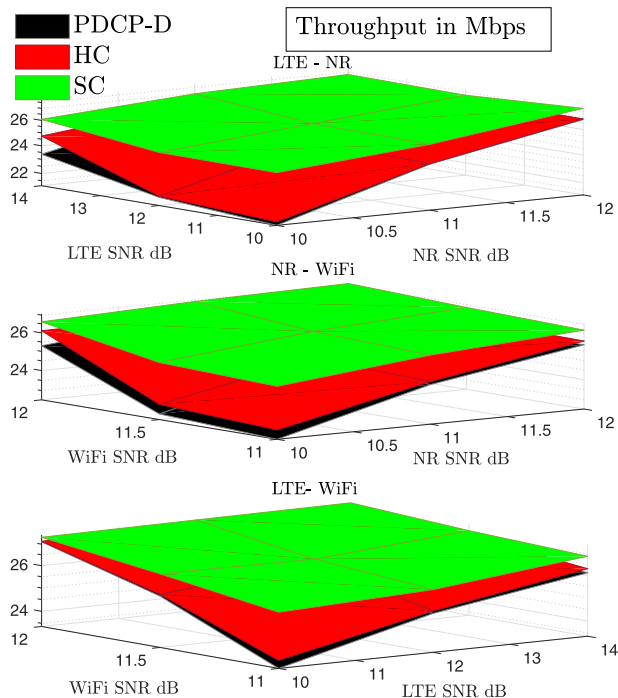
FIGURE 9. The throughput of the combined system (in Mbps) as per simulation parameters listed in Table 3.

based duplication scheme, if both the paths fail to decode the block successfully, then a block-error is declared. By contrast, in our schemes combining is initiated when both paths fail. From this argument and the Table, we conclude that combining rectifies errors in such blocks, which otherwise could not be corrected using coding. Thus, we can view our scheme as an intermediate step in a three-step HARQ process. In the first step, we do CRC, then combining and finally FEC. This three-step procedure reduces the BLER and improves the throughput as shown in Fig. 9, which plots the throughput for three sub-scenarios of Scenario-2. The throughput is also summarized in Table 10.

X. CONCLUSIONS AND FUTURE WORK
In this work, we propose a new L2 layer-based diversity scheme, combining that the next-generation networks can adopt to enhance reliability. When the CRC and FEC procedures fail, the proposed scheme optimally combines the RLC PDUs arriving at the UE from various MAC entities. It is the first time an optimal MAC level diversity combining scheme is proposed to the best of our knowledge. Simulations demonstrate that optimally combined PDUs reduce the block error rates substantially. Moreover, the average latency is also improved in various interest regimes, especially when SNR for a given MCS is low. The scheme can certainly help design strategies beyond 5G networks by combining the essential 5G advantages with this cross-layer technique.

In the future, it will be of much interest to investigate multi-RAT and multi-connectivity based solutions to tackle the rising demand for bandwidth. The main challenge will be

to ensure latency below the prescribed limits. Another challenge is to evaluate the performance comparison of the hard-combining scheme with the selection-combining scheme for multi-connectivity with more than two connected paths.

APPENDIX A
DESCRAMBLING OF LLRs
To obtain the LLRs of the descrambled bits, $LLR(c_{i,j})$, the receiver employs a soft-descrambling procedure described as follows. The receiver determines the descrambler's initial state based on set rules in a standard and obtains the corresponding pseudo-random sequence. Since the LLRs are available only at the pre-descrambling stage, the LLRs of scrambled bits are used to obtain LLRs for descrambled bits. To do so, observe the following. The likelihood ratio of a scrambled bit $\tilde{c}_{i,j}$ is

$$\Lambda(\tilde{c}_{i,j}) = \frac{Pr(\tilde{c}_{i,j} = 1|y)}{Pr(\tilde{c}_{i,j} = 0|y)} \tag{23}$$

Also note that $\tilde{c}_{i,j} = c_{i,j} \oplus s_{i,j}$, where $s_{i,j}$ is the binary element of the scrambling sequence that is used to scramble bit j in the $i-$th channel. Thus we have $c_{i,j} = \tilde{c}_{i,j} \oplus s_{i,j}$.

Now,

$$\Lambda(c_{i,j}) = \frac{Pr(c_{i,j} = 1|y)}{Pr(c_{i,j} = 0|y)} \tag{24}$$

$$= \frac{Pr(\tilde{c}_{i,j} \oplus s_{i,j} = 1|y = 0)}{Pr(\tilde{c}_{i,j} \oplus s_{i,j} = 0|y = 0)} \tag{25}$$

Thus if $s_{i,j} = 0$, then

$$\Lambda(c_{i,j}) = \frac{Pr(\tilde{c}_{i,j} = 1|y)}{Pr(\tilde{c}_{i,j} = 0|y)} = \Lambda(\tilde{c}_{i,j}), \tag{26}$$

whereas if $s_{i,j} = 1$, then

$$\Lambda(c_{i,j}) = \frac{Pr(\tilde{c}_{i,j} = 0|y)}{Pr(\tilde{c}_{i,j} = 1|y)} = \frac{1}{\Lambda(\tilde{c}_{i,j})} \tag{27}$$

Finally, $LLR(c_{i,j}) = \ln \Lambda(c_{i,j})$.

APPENDIX B
PROBABILITY OF BIT-ERROR FOR WELL KNOWN DISTRIBUTIONS
For BPSK signalling with slow Rayleigh fading we have [70],

$$p_i = \frac{1}{2}\left[1 - \sqrt{\frac{\bar{\gamma}_{b,i}}{2 + \bar{\gamma}_{b,i}}}\right], \tag{28}$$

while for Rician fading we have,

$$p_i = \frac{1}{\pi}\int_0^{\pi/2} \frac{(\kappa+1)\sin^2\theta}{\bar{\gamma}_{b,i} + (\kappa+1)\sin^2\theta} e^{\left(-\frac{\bar{\gamma}_{b,i}\kappa}{(\kappa+1)\sin^2\theta + \bar{\gamma}_{b,i}}\right)} d\theta. \tag{29}$$

where κ is the ratio between the power received in the Line-of-Sight path to the power received in the other paths[4]. For

[4]For a carefull study of Fading distributions one may read either of [63], [70], [71]

the Nakagami-m fading, $m \in \{1, 2, \ldots\}$ we have

$$p_i = \frac{1}{2} - \frac{\tilde{\sigma}}{2} \sum_{i=0}^{m-1} \left(\frac{m\tilde{\sigma}^2}{4\bar{\gamma}_{b,i}} \right)^i \frac{(2i)!}{(i!)^2} \quad (30)$$

where $\tilde{\sigma} = \sqrt{\dfrac{\bar{\gamma}_{b,i}}{(\bar{\gamma}_{b,i} + m)}}$.

APPENDIX C
PROOF OF LEMMA 3
To begin with, we have

$$q(i) = \Pr\left\{ \sum_{j=1}^{N} |H_j|^2 (2\hat{b}_j - 1) > 0 \Big| \hat{b}_i = 0, b = 1 \right\} p_i \quad (31)$$

$$r(i) = \Pr\left\{ \sum_{j=1}^{N} |H_i|^2 (2\hat{b}_j - 1) > 0 \Big| \hat{b}_i = 0, b = 0 \right\} (1 - p_i) \quad (32)$$

We calculate q_i as follows. Let $\mathcal{S} = \{1, 2, \ldots, N\}$ and let $\mathcal{S}_{-i} = \{1, 2, \ldots, i-1, i+1, \ldots, N\}$. In what follows now we drop the subscript used for indicating the bit number. For example, in $H_{i,j}$, i indicated the MAC entity and j, the bit number in a block. We now mention simply H_i because probability of bit error is identical over $j = \{1, \ldots, N_M\}$. Now consider the probability

$$\Pr\left\{ \sum_{j=1}^{N} |H_j|^2 (2\hat{b}_j - 1) > 0 | \hat{b}_i = 0, b = 1 \right\}$$
$$= \Pr\left\{ \sum_{j\in\mathcal{S}_{-i}} |H_j|^2 (2\hat{b}_j - 1) > |H_i|^2|, b = 1 \right\} \quad (33)$$

Notice that we have removed the condition $\hat{b}_i = 0$ because it is now incorporated in the probability calculation. Since $\hat{b}_j \in \{0, 1\}$, $j \in \mathcal{S}_{-i}$ we condition the above probability on every possible combination of b_j's over $j \in \mathcal{S}_{-i}$. Consider the power set $2^{\mathcal{S}_{-i}}$ of $\mathcal{S}_{-i}$ that contains all the subsets of S_{-i}. Each element in the power set indicates one possible combination of b_j's. That is, consider $\mathcal{P}_i \in 2^{\mathcal{S}_{-i}}$. Since a power set is closed under complementation, $\mathcal{P}_i^c \in 2^{\mathcal{S}_{-i}}$. Let $\hat{b}_j = 1$ if $j \in \mathcal{P}_i$. Running over all possible $\mathcal{P}_i \in 2^{\mathcal{S}_{-i}}$, we cover every scenario. Note that different $\mathcal{P}_i$ represent disjoint combinations of b_j. Denote $\boldsymbol{b}_{-i} = \{\hat{b}_1, \hat{b}_2, \ldots, \hat{b}_{i-1}, \hat{b}_{i+1}, \ldots, \hat{b}_N\}$. Let $\boldsymbol{b}_{\mathcal{P}_i}$ be the $N-1$ length vector with $k-$ element 1 if $k \in \mathcal{P}_i$ and zero otherwise. Let $\tilde{\mathcal{P}}_i^c = \mathcal{P}_i^c \cup \{i\}$. Then the RHS of (33) becomes

$$\sum_{\mathcal{P}_i \in 2^{\mathcal{S}_{-i}}} \left[\Pr\left\{ \sum_{j\in\mathcal{P}_i} |H_j|^2 > \sum_{j\in\tilde{\mathcal{P}}_i^c} |H_j|^2 \Big| \boldsymbol{b}_{-i} = \boldsymbol{b}_{\mathcal{P}_i}, b = 1 \right\} \right.$$
$$\left. \times \Pr\{\boldsymbol{b}_{-i} = \boldsymbol{b}_{\mathcal{P}_i} | b = 1\} \right]. \quad (34)$$

For a fixed b, the $\hat{b}_j$'s are independent, and hence

$$\Pr\{\boldsymbol{b}_{-i} = \boldsymbol{b}_{\mathcal{P}_i} | b = 1\} = \prod_{j\in\mathcal{P}_i} \prod_{k\in\mathcal{P}_i^c} p_j(1 - p_k). \quad (35)$$

Thus (34) reduces to

$$\sum_{\mathcal{P}_i \in 2^{\mathcal{S}_{-i}}} \left[\Pr\left\{ \sum_{j\in\mathcal{P}_i} |H_j|^2 > \sum_{j\in\tilde{\mathcal{P}}_i^c} |H_j|^2 \Big| \boldsymbol{b}_{-i} = \boldsymbol{b}_{\mathcal{P}_i}, b = 1 \right\} \right.$$
$$\left. \times \prod_{j\in\mathcal{P}_i} \prod_{k\in\mathcal{P}_i^c} p_j(1 - p_k) \right]$$
$$= \sum_{\mathcal{P}_i \in 2^{\mathcal{S}_{-i}}} \left[\Pr\left\{ \sum_{j\in\mathcal{P}_i} |H_j|^2 > \sum_{j\in\tilde{\mathcal{P}}_i^c} |H_j|^2 \right\} \right.$$
$$\left. \times \prod_{j\in\mathcal{P}_i} \prod_{k\in\mathcal{P}_i^c} p_j(1 - p_k) \right] \quad (36)$$

Notice that the conditioning in the first factor is no more required as we have incorporated its effect in the probability calculation. The $\Pr\left\{ \sum_{j\in\mathcal{P}_i} |H_j|^2 > \sum_{j\in\tilde{\mathcal{P}}_i^c} |H_j|^2 \right\}$ will depend upon the distribution of $|H_j|^2$. For Rayleigh fading $|H_j|^2$ is exponentially distributed. Certainly $|H_j|^2$ are independent over i, but are not identical, because we have a Multi-RATs system and such an assumption will, in general, not hold. However, it is clear that if they were indeed identical then the r.v.s $\sum_{j\in\mathcal{P}_i} |H_j|^2$ and $\sum_{j\in\tilde{\mathcal{P}}_i^c} |H_j|^2$ both the follow the Erlang distribution [72] but with different parameters. So if $\mathbb{E}[|H_j|^2] = \lambda$ and $|\mathcal{S}|$ is the number of elements in the set $\mathcal{S}$, then $\sum_{j\in\mathcal{P}_i} |H_j|^2 \sim \text{Erlang}(\lambda, |\mathcal{P}_i|)$ while $\sum_{j\in\tilde{\mathcal{P}}_i^c} |H_j|^2 \sim \text{Erlang}(\lambda, |\tilde{\mathcal{P}}_i^c|)$, where $\text{Erlang}(\alpha, n)$ is has the following density

$$f_E(x, \alpha, n) = \frac{\alpha^k x^{n-1} e^{-\alpha x}}{(n-1)!} \quad \text{for } x, \alpha \geq 0 \quad (37)$$

Thus,

$$\Pr\left\{ \sum_{j\in\mathcal{P}_i} |H_j|^2 > \sum_{j\in\tilde{\mathcal{P}}_i^c} |H_j|^2 \right\} \quad (38)$$
$$= \int_{x=0}^{\infty} \int_{y=0}^{x} f_E(y, \lambda, |\tilde{\mathcal{P}}_i^c|) f_E(x, \lambda, |\mathcal{P}_i|) dy dx. \quad (39)$$

We can now state the result for $q(i)$. Also on similar lines we can derive the probability for $r(i)$. For this purposed let $\tilde{\mathcal{P}}_i = \mathcal{P}_i \bigcup \{i\}$. The Lemma then follows.

APPENDIX D
PROOF OF LEMMA 4
For the case when $|H_j|^2$ are independent and exponentially distributed but with distinct mean, say $\mathbb{E}[|H_j|^2] = \lambda_j$, let $\boldsymbol{\lambda}_{\mathcal{P}_i} = \{\lambda_j : j \in \mathcal{P}_i\}$. Instead of Erlang distribution, we will now call the resulting distribution as the modified Erlang or M-Erlang distribution. Note that this distribution will take all the distinct mean values inputs. Then $\sum_{j\in\mathcal{P}_i} |H_j|^2 \sim \text{M-Erlang}(\boldsymbol{\lambda}_{\mathcal{P}_i}, |\mathcal{P}_i|)$ and $\sum_{j\in\tilde{\mathcal{P}}_i^c} |H_j|^2 \sim \text{M-Erlang}(\boldsymbol{\lambda}_{\tilde{\mathcal{P}}_i^c}, |\tilde{\mathcal{P}}_i^c|)$, where the density of

the M-Erlang($\{\beta_1, \ldots, \beta_n\}, n$) is as follows [73]:

$$f_{EM}(x; (\{\beta_1, \ldots, \beta_n\}, n)) = \sum_{k=1}^{n} \frac{\beta_1 \cdots \beta_n}{\prod_{\substack{j=1 \\ j \neq k}}^{n} (\beta_j - \beta_k)} e^{(-x\beta_k)}$$

(40)

where $\beta_j > 0 \; \forall j$ and $x > 0$. The Lemma then follows

APPENDIX E
PROOF OF LEMMA 1

The LLR for b_j,

$$LLR(b_j) = \ln\left(\frac{f_X(X_j = 1 | Y_j, H_j)}{f_X(X_j = -1 | Y_j, H_j)}\right), \quad (41)$$

This is for BPSK modulation which can be extended (non-trivially) to higher order modulation schemes.

$$\frac{f_X(X_j = 1 | Y_j, H_j)}{f_X(X_j = -1 | Y_j, H_j)} = \frac{f(Y_j | H_j, X_j = 1)}{f(Y_j | H_j, X_j = -1)}. \quad (42)$$

The noise $Z_{i,j}$ is Gaussian, independent and identically distributed over time and paths. Thus given X_j and the estimate of $H_{i,j}$ at the receiver, $Y_{i,j}$s are independent over i. Thus,

$$\frac{f(Y_j | H_j, X_j = 1)}{f(Y_j | H_j, X_j = -1)} = \frac{\exp\left(-\sum_{i=1}^{N} \frac{|Y_{i,j} - H_{i,j}|^2}{\sigma_i^2}\right)}{\exp\left(-\sum_{i=1}^{N} \frac{|Y_{i,j} + H_{i,j}|^2}{\sigma_i^2}\right)}$$

The LLR thus becomes,

$$LLR(b_j) = 2 \sum_{i=1}^{N} \frac{\Re\{Y_{i,j} H_{i,j}^*\}}{\sigma_i^2} \quad (43)$$

Note that $2 \frac{\Re\{Y_{i,j} H_{i,j}^*\}}{\sigma_i^2} = LLR(b_{i,j})$. Thus the optimal combining rule is $LLR(b_j) = \sum_{i=1}^{N} LLR(b_{i,j})$ and the decoding strategy is

$$\hat{b}_j = \begin{cases} 0 & \text{if, } LLR(b_j) < 0 \\ 1 & \text{otherwise.} \end{cases} \quad (44)$$

APPENDIX F
PROOF OF LEMMA 2

Since the bits 0 and 1 are equiprobable, the probability of error for hard-combining (5) is,

$$p_{e,h} = P(\hat{b}_j \neq 1 | b_j = 0) = P(L\hat{L}R(b_j) > 0 | b_j = 0)$$

$$= P(\sum_{i=1}^{2} |H_{i,j}|^2 (2\hat{b}_{i,j} - 1) > 0 | b_j = 0)$$

$$= P\left(|H_{1,j}|^2 > |H_{2,j}|^2\right) P(\hat{b}_{1,j} = 1 | b_j = 0)$$
$$\times P(\hat{b}_{2,j} = 0 | b_j = 0)$$
$$+ P(|H_{1,j}|^2 < |H_{2,j}|^2) P(\hat{b}_{1,j} = 0 | b_j = 0)$$
$$\times P(\hat{b}_{2,j} = 1 | b_j = 0)$$
$$+ P(\hat{b}_{1,j} = 1 | b_j = 0) P(\hat{b}_{2,j} = 1 | b_j = 0)$$

$$= \gamma p_1 (1 - p_2) + (1 - \gamma_1)(1 - p_1)p_2 + p_1 p_2$$
$$= \gamma p_1 + (1 - \gamma)p_2. \quad (45)$$

Here $\gamma = P(|H_{1,j}|^2 > |H_{2,j}|^2)$, $p_1 = P(\hat{b}_{1,j} = 1 | b_j = 0)$, and $p_2 = P(\hat{b}_{2,j} = 1 | b_j = 0)$. Now, the probability of error for selection-combining is

$$p_{e,s} = P(|H_{1,j}|^2 > |H_{2,j}|^2) P(\hat{b}_{1,j} = 1 | b_j = 0)$$
$$+ P(|H_{1,j}|^2 < |H_{2,j}|^2) P(\hat{b}_{2,j} = 1 | b_j = 0)$$
$$= \gamma p_1 + (1 - \gamma)p_2. \quad (46)$$

Thus $p_{e,h} = p_{e,s}$ for $N = 2$.

APPENDIX G
PROOF OF LEMMA 5

The proof the of Lemma 5 follows from successively conditioning the probability. First $K_i - C_i + E_i$ is conditioned on $K_i = k_i$, $k_i \geq t_i + 1$. Then for each $K_i = k_i$, we are left with the r.v. $E_i - C_i$ and we calculate the probability that $C_i - E_i \geq k_i - t_i$, for which we again condition on $E_i = e_i$. Then for each $K_i = k_i$ and $E_i = e_i$ we are left with the r.v. C_i and we calculate the probability that $C_i \geq k_i + e_i - t_i$. Since C_i can take a maximum value of k_i, it is a binomial r.v. with k_i trials with probability of success q_i. The probability mass function (pmf) of this is exactly $G(c_i; k_i, q_i)$. To correct errors $c_i \in \{k_i + e_i - t_i, \ldots, k_i\}$. For this set to be non-zero, we must have $e_i \leq t_i$ as argued below.

Now, E_i ranges from 0 to $N_m - k_i$, it is also a binomial r.v. with $N_m - k_i$ trial with probability of success r_i. The pmf of E_i is thus $G(e_i; N_M - k_i, r_i)$. The limits of sum on e_i are from 0 to $\min(N_M - k_i, t_i)$ for the following reason. Notice that the minimum number of errors that the super-MAC has to correct to declare an error free block at MAC_i is $C_i = K_i + E_i - t_i$. But this number can at-most be K_i and thus, if $E_i \geq t_i$, then combining fails to correct the block. Thus the maximum value of E_i to correct the block-error is $\min(t_i, N_M - k_i)$.

Finally, K_i is a binomial r.v. with N_M trials with probability of success p_i. The pmf for this is $G(k_i; N_M, p_i)$. Since the super-MAC initiates combining for $K_i \geq t_i + 1$, the limits of the sum on k_i are from $t_i + 1$ to N_M.

REFERENCES

[1] H.-J. Kwon, J. Jeon, A. Bhorkar, Q. Ye, H. Harada, Y. Jiang, L. Liu, S. Nagata, B. L. Ng, T. Novlan, J. Oh, and W. Yi, "Licensed-assisted access to unlicensed spectrum in LTE release 13," *IEEE Commun. Mag.*, vol. 55, no. 2, pp. 201–207, Feb. 2017.

[2] M. Labib, V. Marojevic, J. H. Reed, and A. I. Zaghloul, "Extending LTE into the unlicensed spectrum: Technical analysis of the proposed variants," *IEEE Commun. Standards Mag.*, vol. 1, no. 4, pp. 31–39, Dec. 2017.

[3] R. Bajracharya, R. Shrestha, Y. B. Zikria, and S. W. Kim, "LTE in the unlicensed spectrum: A survey," *IETE Tech. Rev.*, vol. 35, no. 1, pp. 78–90, Jan. 2018.

[4] *Evolved Universal Terrestrial Radio Access (E-UTRA) and Evolved Universal Terrestrial Radio Access Network (E-UTRAN) Overall Description Stage 2*, Standard TS 36.300 version 14.3.0 release 14, 3GPP, Jun. 2017.

[5] A. Garcia-Saavedra, P. Patras, V. Valls, X. Costa-Perez, and D. J. Leith, "ORLA/OLAA: Orthogonal coexistence of LAA and WiFi in unlicensed spectrum," *IEEE/ACM Trans. Netw.*, vol. 26, no. 6, pp. 2665–2678, Dec. 2018.

[6] C. Cano, D. J. Leith, A. Garcia-Saavedra, and P. Serrano, "Fair coexistence of scheduled and random access wireless networks: Unlicensed LTE/WiFi," *IEEE/ACM Trans. Netw.*, vol. 25, no. 6, pp. 3267–3281, Dec. 2017.

[7] X. Sun and L. Dai, "Towards fair and efficient spectrum sharing between LTE and WiFi in unlicensed bands: Fairness-constrained throughput maximization," *IEEE Trans. Wireless Commun.*, vol. 19, no. 4, pp. 2713–2727, Apr. 2020.

[8] Y. Gao and S. Roy, "Achieving proportional fairness for LTE-LAA and Wi-Fi coexistence in unlicensed spectrum," *IEEE Trans. Wireless Commun.*, vol. 19, no. 5, pp. 3390–3404, May 2020.

[9] U. Challita, L. Dong, and W. Saad, "Proactive resource management for LTE in unlicensed spectrum: A deep learning perspective," *IEEE Trans. Wireless Commun.*, vol. 17, no. 7, pp. 4674–4689, Jul. 2018.

[10] H. Cui, V. C. M. Leung, S. Li, and X. Wang, "LTE in the unlicensed band: Overview, challenges, and opportunities," *IEEE Wireless Commun.*, vol. 24, no. 4, pp. 99–105, Aug. 2017.

[11] R. Liu, Q. Chen, G. Yu, G. Y. Li, and Z. Ding, "Resource management in LTE-U systems: Past, present, and future," *IEEE Open J. Veh. Technol.*, vol. 1, pp. 1–17, 2020.

[12] G. Naik, J.-M. Park, J. Ashdown, and W. Lehr, "Next generation Wi-Fi and 5G NR-U in the 6 GHz bands: Opportunities and challenges," *IEEE Access*, vol. 8, pp. 153027–153056, 2020.

[13] N. Patriciello, S. Lagen, B. Bojovic, and L. Giupponi, "NR-U and IEEE 802.11 technologies coexistence in unlicensed mmWave spectrum: Models and evaluation," *IEEE Access*, vol. 8, pp. 71254–71271, 2020.

[14] Y. Jiang, J. Guo, and Z. Fei, "Performance analysis of the coexistence of 5G NR-unlicensed and Wi-Fi with mode selection," in *Proc. IEEE/CIC Int. Conf. Commun. China (ICCC)*, Aug. 2020, pp. 953–958.

[15] D. Laselva, D. Lopez-Perez, M. Rinne, and T. Henttonen, "3GPP LTE-WLAN aggregation technologies: Functionalities and performance comparison," *IEEE Commun. Mag.*, vol. 56, no. 3, pp. 195–203, Mar. 2018.

[16] *Evolved Universal Terrestrial Radio Access (E-UTRA); Physical Layer Procedures*, Standard TS 36.213 Version 13.0.0 Release 13, 3GPP, 2017.

[17] R. Bajracharya, R. Shrestha, R. Ali, A. Musaddiq, and S. W. Kim, "LWA in 5G: State-of-the-Art architecture, opportunities, and research challenges," *IEEE Commun. Mag.*, vol. 56, no. 10, pp. 134–141, Oct. 2018.

[18] H.-L. Maattanen, G. Masini, M. Bergstrom, A. Ratilainen, and T. Dudda, "LTE-WLAN aggregation (LWA) in 3GPP release 13 & release 14," in *Proc. IEEE Conf. Standards for Commun. Netw. (CSCN)*, Sep. 2017, pp. 220–226.

[19] S. Singh, M. Geraseminko, S.-P. Yeh, N. Himayat, and S. Talwar, "Proportional fair traffic splitting and aggregation in heterogeneous wireless networks," *IEEE Commun. Lett.*, vol. 20, no. 5, pp. 1010–1013, May 2016.

[20] B. Chen, N. Pappas, Z. Chen, D. Yuan, and J. Zhang, "Throughput and delay analysis of LWA with bursty traffic and randomized flow splitting," *IEEE Access*, vol. 7, pp. 24667–24678, 2019.

[21] Y.-B. Lin, Y.-J. Shih, and P.-W. Chao, "Design and implementation of LTE RRM with switched LWA policies," *IEEE Trans. Veh. Technol.*, vol. 67, no. 2, pp. 1053–1062, Feb. 2018.

[22] Y.-K. Tu, C.-H. Lee, C.-H. Liu, C.-Y. Chia, Y.-K. Chen, and Y.-B. Lin, "Deployment of the first commercial LWA service," *IEEE Wireless Commun.*, vol. 24, no. 6, pp. 6–8, Dec. 2017.

[23] H. Liu, Y. Liu, F. Yang, and P. Chen, "A SDR-based NR-WLAN aggregation system towards 5G indoor coverage," in *Proc. IEEE 5th Int. Conf. Comput. Commun. (ICCC)*, Dec. 2019, pp. 1023–1029.

[24] Y. Ohta, R. Takechi, H. Takahashi, and R. Atsuta, "NR-WLAN aggregation: Architecture for supporting URLLC in 5G IoT networks," in *Proc. IEEE 91st Veh. Technol. Conf. (VTC-Spring)*, May 2020, pp. 1–5.

[25] *LTE/WLAN Radio Level Integration using IPsec Tunnel (LWIP) Encapsulation*, Standard TS 36.361, 3GPP, Apr. 2016.

[26] D. Lopez-Perez, J. Ling, B. H. Kim, V. Subramanian, S. Kanugovi, and M. Ding, "LWIP and Wi-Fi boost flow control," in *Proc. IEEE Wireless Commun. Netw. Conf. (WCNC)*, Mar. 2017, pp. 1–6.

[27] X. Zhu, K. Chen, X. Zhang, and M. Chen, "Simulation design and performance evaluation of LWIP system," in *Proc. 10th Int. Conf. Educ. Technol. Comput. (ICETC)*, 2018, pp. 369–373.

[28] J. F. Monserrat, F. Bouchmal, D. Martin-Sacristan, and O. Carrasco, "Multi-radio dual connectivity for 5G small cells interworking," *IEEE Commun. Standards Mag.*, vol. 4, no. 3, pp. 30–36, Sep. 2020.

[29] O. N. C. Yilmaz, O. Teyeb, and A. Orsino, "Overview of LTE-NR dual connectivity," *IEEE Commun. Mag.*, vol. 57, no. 6, pp. 138–144, Jun. 2019.

[30] *5G NR–Packet Data Convergence Protocol (PDCP) Specification*, Standard TS 38.323 version 15.2.0 release 15, 3GPP, Sep. 2018.

[31] P. J. D. Chandramouli and R. Liebhart, *5G for the Connected World*. Hoboken, NJ, USA: Wiley, Apr. 2019.

[32] D. S. Michalopoulos and V. Pauli, "Data duplication for high reliability: A protocol-level simulation assessment," in *Proc. IEEE Int. Conf. Commun. (ICC)*, May 2019, pp. 1–7.

[33] M. Centenaro, D. Laselva, J. Steiner, K. Pedersen, and P. Mogensen, "System-level study of data duplication enhancements for 5G downlink URLLC," *IEEE Access*, vol. 8, pp. 565–578, 2020.

[34] D. Vukobratovic, A. Tassi, S. Delic, and C. Khirallah, "Random linear network coding for 5G mobile video delivery," *Information*, vol. 9, no. 4, p. 72, Mar. 2018.

[35] N. H. Mahmood and H. Alves, "Dynamic multi-connectivity activation for ultra-reliable and low-latency communication," in *Proc. 16th Int. Symp. Wireless Commun. Syst. (ISWCS)*, Aug. 2019, pp. 112–116.

[36] M. Centenaro, D. Laselva, J. Steiner, K. Pedersen, and P. Mogensen, "Resource-efficient dual connectivity for ultra-reliable low-latency communication," in *Proc. IEEE 91st Veh. Technol. Conf. (VTC-Spring)*, May 2020, pp. 1–5.

[37] A. Aijaz, "Packet duplication in dual connectivity enabled 5G wireless networks: Overview and challenges," *IEEE Commun. Standards Mag.*, vol. 3, no. 3, pp. 20–28, Sep. 2019.

[38] P. Sharma, A. Brahmakshatriya, T. V. Pasca S, B. R. Tamma, and A. Franklin, "LWIR: LTE-WLAN integration at RLC layer with virtual WLAN scheduler for efficient aggregation," in *Proc. IEEE Global Commun. Conf. (GLOBECOM)*, Dec. 2016, pp. 1–6.

[39] E. Pei, D. Meng, L. Li, and P. Zhang, "Performance analysis of listen before talk based coexistence scheme over the unlicensed spectrum in the scenario with multiple LTE small bases," *IEEE Access*, vol. 5, pp. 10364–10368, 2017.

[40] V. Mushunuri, B. Panigrahi, H. K. Rath, and A. Simha, "Fair and efficient listen before talk (LBT) technique for LTE licensed assisted access (LAA) networks," in *Proc. IEEE 31st Int. Conf. Adv. Inf. Netw. Appl. (AINA)*, Mar. 2017, pp. 39–45.

[41] *Evolved Universal Terrestrial Radio Access (E-UTRA) and Eolved Universal Terrestrial Radio Access Network (E-UTRAN) Overall Description Stage 2*, Standard TS 36.300 Version 13.2.0 Release 13, 3GPP, Jan. 2016.

[42] *LTE Study on Licensed-Assisted Access to Unlicensed Spectrum*, Standard 3GPP 4G, (Release 13), Jul. 2015.

[43] *NR Study on NR-Based Access to Unlicensed Spectrum*, Standard G. T. 38.889 5G, (Release 16), Dec. 2018.

[44] V. Maglogiannis, D. Naudts, A. Shahid, and I. Moerman, "An adaptive LTE listen-before-talk scheme towards a fair coexistence with Wi-Fi in unlicensed spectrum," *Telecommun. Syst.*, vol. 68, no. 4, pp. 701–721, Aug. 2018.

[45] V. A. Loginov, A. I. Lyakhov, and E. M. Khorov, "Coexistence of Wi-Fi and LTE-LAA networks: Open issues," *J. Commun. Technol. Electron.*, vol. 63, no. 12, pp. 1530–1537, Dec. 2018.

[46] *MulteFire Release 1.1 Technical Overview White Paper*, MulteFire Alliance, Fremont, CA, USA, Nov. 2019.

[47] A. Nordrum, "Intel, Nokia, qualcomm bet on multere to blend LTE and WiFi," *Tech-Talk*. [Online]. Available: https://spectrum.ieee.org/techtalk/telecom/wireless/intel-nokia-qualcomm-betting-on-multefire-to-blend-lte-and-wifi

[48] B. Ismaiel, M. Abolhasan, D. Smith, W. Ni, and D. Franklin, "A survey and comparison of device-to-device architecture using LTE unlicensed band," in *Proc. IEEE 85th Veh. Technol. Conf. (VTC Spring)*, Jun. 2017, pp. 1–5.

[49] C. Rosa, M. Kuusela, F. Frederiksen, and K. I. Pedersen, "Standalone LTE in unlicensed spectrum: Radio challenges, solutions, and performance of MulteFire," *IEEE Commun. Mag.*, vol. 56, no. 10, pp. 170–177, Oct. 2018.

[50] R. Sun, S. Talarico, W. Chang, H. Niu, and H. Yang, "Enabling NB-IoT on unlicensed spectrum," in *Proc. IEEE 30th Annu. Int. Symp. Pers., Indoor Mobile Radio Commun. (PIMRC)*, Sep. 2019, pp. 1–7.

[51] C.-W. Hsu, K. Das, and L. Jorguseski, "Multi-RAT random access scheme utilising combined licensed and unlicensed spectrum for massive machine-type communications," in *Proc. IEEE 91st Veh. Technol. Conf. (VTC-Spring)*, May 2020, pp. 1–7.

[52] *LTE Evolved Universal Terrestrial Radio Access Network (E-UTRAN) and Wireless Local Area Network (WLAN); Xw Interface User Plane Protocol*, Standard TS 36.465 Version 13.2.0 Release 13, 3GPP, Sep. 2017.

[53] *LTE; Evolved Universal Terrestrial Radio Access Network (EUTRAN) and Wireless LAN (WLAN); Xw Data Transport*, Standard TS 36.464 Version 14.0.0 Release 14, 3GPP, Apr. 2017.

[54] *LTE; Evolved Universal Terrestrial Radio Access (E-UTRA); Packet Data Convergence Protocol (PDCP) Specification*, Standard TS 36.323 Version 13.6.0 Release 13, 3GPP, Jun. 2017.

[55] *LTE; Evolved Universal Terrestrial Radio Access (E-UTRA); LTE-WLAN Aggregation Adaptation Protocol (LWAAP) Specification*, Standard TS 36.360 Version 13.1.0 Release 13, 3GPP, Jun. 2017.

[56] S. Sirotkin, "LTE-WLAN aggregation (LWA): Benefits and deployment considerations," Next Gener. Standards Group, Intel Corp., Frankfurt, Germany, White Paper 2016. [Online]. Available: https://www.intel.com/content/dam/www/public/us/en/documents/white-papers/lte-wlan-aggregation-deployment-paper.pdf

[57] *LTE; Evolved Universal Terrestrial Radio Access (E-UTRA); LTE-WLAN Radio Level Integration using IPsec Tunnel (LWIP) Encapsulation. Protocol Specification*, Standard TS 36.361 version 13.2.0 release 13, 3GPP, Oct. 2016.

[58] *5G;NG Radio Access Network (NG-RAN);Stage 2 Functional Specification of User Equipment (UE) Positioning in NG-RAN*, Standard TS 38.305 Version 15.1.0 Release 15), 3GPP, 2017.

[59] E. W. Jang, J. Lee, H.-L. Lou, and J. M. Cioffi, "On the combining schemes for MIMO systems with hybrid ARQ," *IEEE Trans. Wireless Commun.*, vol. 8, no. 2, pp. 836–842, Feb. 2009.

[60] G. R. Woo, P. Kheradpour, D. Shen, and D. Katabi, "Beyond the bits: Cooperative packet recovery using physical layer information," in *Proc. 13th Annu. ACM Int. Conf. Mobile Comput. Netw.*, New York, NY, USA: Association for Computing Machinery, 2007, pp. 147–158.

[61] S. S. Chakraborty, E. Yli-Juuti, and M. Liinaharja, "An ARQ scheme with packet combining," *IEEE Commun. Lett.*, vol. 2, no. 7, pp. 200–202, Jul. 1998.

[62] P. Frenger, S. Parkvall, and E. Dahlman, "Performance comparison of HARQ with Chase combining and incremental redundancy for HSDPA," in *Proc. IEEE 54th Veh. Technol. Conf.*, vol. 3, Oct. 2001, pp. 1829–1833.

[63] D. Tse and P. Viswanath, *Fundamentals ofWireless Communication*. Cambridge, U.K.: Cambridge Univ. Press, 2005.

[64] *5G–NR Study on Scenarios and Requirements for Next Generation Access Technologies*, Standard TR 38.913 version 14.2.0 release 14, 3GPP, May 2017.

[65] *4G–LTE Feasibility Study for Further Advancements for E-UTRA (LTE-Advanced)*, Standard TR 36.912 version 14.0.0 Release 14, 3GPP, Apr. 2017.

[66] "4G-5G interworking; RAN-level and CN-level interworking," Samsung, Seoul, South Korea, White Paper, Jun. 2017. [Online]. Available: https://images.samsung.com/is/content/samsung/p5/global/business/networks/insights/white-paper/4g-5g-interworking/global-networks-insight-4g-5g-interworking-0.pdf

[67] *IEEE Standard for Information Technology, Part 11: WLAN MAC and PHY specifications: Enhancements for Very High Throughput for Operation in Bands below 6 GHz*, Standard 802.11ac(TM)-2013, 2013, pp. 1–425.

[68] *5G–NR User Equipment (UE) Radio Access Capabilities*, Standard TS 38.306 version 15.3.0 release 15, 3GPP, Oct. 2018.

[69] *5G–NR Physical Channels and Modulation*, Standard TS 38.211 version 15.2.0 release 15, 3GPP, Jul. 2018.

[70] V. V. Veeravalli, *Lecture Notes in Wireless Communications*. London, U.K.: Fall 2007.

[71] A. Goldsmith, *Wireless Communications*. Cambridge, U.K.: Cambridge Univ. Press, 2005.

[72] D. R. Cox, *Renewal Theory*. London, U.K.: Wiley, 1962.

[73] M. Akkouchi, "On the convolution of exponential distributions," *J. Chungcheong Math. Soc.*, vol. 21, no. 4, pp. 501–510, Dec. 2008.

ABDUL MATEEN AHMED (Graduate Student Member, IEEE) is currently a Ph.D. Student with the Department of Electrical Engineering, IIT Hyderabad. Prior to this, he was a Telecom implementation Engineer for Nokia EDGE, 3G, HSDPA, and 4G. Later, he worked with Core Access as a Second level Maintenance Engineer for the STC NSN JV project. He has hands on experience in Mobile networks for Nokia BTS, BSC, TCSM, BSC, RNC, eNB, and CWO implementation, integration, and troubleshooting. He has also worked for Nokia, Motorola, and Huawei, Madinah Al-Munawarrah, Saudi Arabia, for nine years. He received the best performer awards for the completion of the Nokia E-5,6 phase, Hajj projects, and Mobily projects. He has a keen research interest in developing efficient algorithms to improve receiver performance on key factors. His Ph.D. thesis focuses on next-generation networks and data-combining schemes through duplication.

AAQIB PATEL (Member, IEEE) received the B.Tech. degree from NIT Warangal, in 2010, and the Ph.D. degree from IIT Bombay, in 2016. He has been a DST INSPIRE Faculty with the Department of Electrical Engineering, IIT Hyderabad, since September 2017. Prior to this position, he was a Project Research Scientist with IIT Hyderabad and IIT Bombay. His Ph.D. thesis has focused on fundamental limits for cognitive radio channels working under practical constraints. Prior to joining IIT Bombay, he had been a Project Trainee with Crompton Greaves Ltd., Mumbai, in summer 2008, where he worked on schemes to optimize the hardware of various producers. He was a Research Intern with IIT Bombay in summer 2009, where he worked on Schemes for Video-Shot Boundary Detection. He has more than four years of experience in research in wireless communications and information theory. He received funding from the DST, GoI, for his INSPIRE Faculty Fellowship. His research interests include cross-layer techniques for 5G and B5G networks, coding for massive MIMO, information theory of wireless networks, and cyber-physical systems.

MOHAMMED ZAFAR ALI KHAN (Senior Member, IEEE) received the B.E. degree in electronics and communications from Osmania University, Hyderabad, India, in 1996, the M.Tech. degree in electrical engineering from IIT Delhi, in 1998, and the Ph.D. degree in electrical communication engineering from IISc, Bengaluru, in 2003. He was a Design Engineer with Sasken, Bengaluru, in 1999, a Senior Design Engineer with Silica Semiconductors, Bengaluru, from 2003 to 2005, a Senior Member of Technical Staff with Hellosoft, India, in 2005, and an Assistant Professor with IIIT Hyderabad from 2006 to 2009. He is currently a Professor with IIT Hyderabad. He has more than 15 years of experience in teaching and research. He has made noteworthy contributions to Space time codes. The Space time block codes designed by him have been adopted by the WiMAX Standard. He has been a chief investigator for a number of sponsored and consultancy projects. He is a reviewer for many international and national journals and conferences. He is the author of book *Single and Double Symbol Decodable Space-Time Block Codes* from Lambert academic press, Germany. His research interests include coded modulation, space-time coding, and signal processing for wireless communications. He was a recipient of INAE Young Engineer Award 2006.

• • •